

Nonenhanced MR Angiography¹

Mitsue Miyazaki, PhD
Vivian S. Lee, MD, PhD

While nonenhanced magnetic resonance (MR) angiographic methods have been available since the earliest days of MR imaging, prolonged acquisition times and image artifacts have generally limited their use in favor of gadolinium-enhanced MR angiographic techniques. However, the combination of recent technical advances and new concerns about the safety of gadolinium-based contrast agents has spurred a resurgence of interest in methods that do not require exogenous contrast material. After a review of basic considerations in vascular imaging, the established methods for nonenhanced MR angiographic techniques, such as time of flight and phase contrast, are considered and their advantages and disadvantages are discussed. This article then focuses on new techniques that are becoming commercially available, such as electrocardiographically gated partial-Fourier fast spin-echo methods and balanced steady-state free precession imaging both with and without arterial spin labeling. Challenges facing these methods and possible solutions are considered. Since different imaging techniques rely on different mechanisms of image contrast, recommendations are offered for which strategies may work best for specific angiographic applications. Developments on the horizon include techniques that provide time-resolved imaging for assessment of flow dynamics by using nonenhanced approaches.

© RSNA, 2008

¹ From the Department of MRI, Toshiba Medical Research Institute USA, 990 Corporate Woods Pkwy, Vernon Hills, IL 60061 (M.M.); and Department of Radiology, New York University Medical Center, New York, NY (V.S.L.). Received August 24, 2007; revision requested November 7; revision received November 30; accepted January 29, 2008; final version accepted February 21. **Address correspondence to** M.M. (e-mail: mmiyazaki@tams.com).

V.S.L., who is not an employee of or consultant to Toshiba, had control of inclusion of any data and information that might present a conflict of interest for M.M., who is an employee of Toshiba.

© RSNA, 2008

Magnetic resonance (MR) angiographic techniques can be divided into two categories: contrast material-enhanced and nonenhanced MR angiography. Since its introduction in 1994 by Prince (1), first-pass contrast-enhanced MR angiography with gadolinium-based contrast material has seen widespread acceptance. The approach has benefited from many technical advances, including strategies to synchronize arrival of the bolus of contrast material with MR acquisition (2–4), moving bed technology for multistation studies such as peripheral MR angiography (5,6), shortened acquisition times with parallel imaging (7), and k-space sharing methods such as time-resolved imaging of contrast kinetics, or TRICKS,

for “time-resolved” MR angiographic acquisitions (8).

Among the nonenhanced techniques that have been available for many years, three-dimensional (3D) time-of-flight (TOF) MR angiography remains the mainstay of intracranial arterial evaluation. For peripheral MR angiography, flow is oriented craniocaudally, and two-dimensional (2D) TOF has been established as an accurate method to diagnose peripheral vascular disease. However, long acquisition times are needed to image from the abdominal aorta to pedal arteries with transverse sections. The requirement for section positioning orthogonal to the direction of flow has precluded application of TOF methods in areas of complex geometry such as the thoracic aorta or renal arteries. Phase-contrast imaging is less commonly used to produce angiographic images because of its relatively long acquisition times (9–12). Until recently, other nonenhanced methods, such as arterial spin labeling (ASL) (13–15), have been confined to research applications.

Several factors contribute to a renaissance of interest in nonenhanced MR angiographic methods. Improvements in MR hardware and software, including the widespread availability of parallel imaging (16,17), have helped reduce acquisition times and made some methods clinically practical. Moreover, the recent association between high doses of gadolinium-based contrast material for MR angiography and the debilitating and occasionally life-threatening entity, nephrogenic systemic fibrosis (18–20), originally known as nephrogenic fibrosing dermopathy, has made it imperative that patients with moderate to severe renal insufficiency and vascular disease have nonenhanced alternatives for angiography. Much of the research on nonenhanced MR angiographic techniques originates in Japan, driven by the relatively high costs and limitations on dosing of contrast material there (21). It is also important to note that nonenhanced MR angiography can play a useful role as a supplement to gadolinium-enhanced MR angiography, particularly when the contrast-enhanced methods fail or have serious artifacts (22).

The purpose of this article is to inform the clinical imager about new horizons in the field of nonenhanced MR angiography. The focus is on arteriographic applications, reserving venography for separate consideration. We begin by summarizing general principles of vascular MR imaging, reviewing the established nonenhanced methods such as TOF and phase-contrast MR angiography (23), and then discussing in greater detail newer strategies for MR angiography that do not require exogenous contrast material, concentrating on electrocardiographically (ECG)-gated partial-Fourier fast spin echo (FSE) and balanced steady-state free precession (SSFP) (also referred to as balanced fast field echo; true fast imaging with steady-state precession, or true FISP; fast imaging employing steady-state acquisition, or FIESTA; true SSFP; among others) with ASL. Finally, the article concludes with a summary of possible strategies for nonenhanced alternatives in specific MR angiographic applications and consideration of future directions.

Essentials

- Improvements in MR hardware and software, coupled with concerns about the safety of gadolinium-based contrast agents, have contributed to a renaissance of interest in nonenhanced MR angiography.
- Time-of-flight MR is widely used for intracranial angiography and, in some centers, for carotid and distal peripheral MR angiography.
- Electrocardiographically (ECG)-gated 3D partial-Fourier fast spin-echo (FSE) methods rely on subtraction of systolic from diastolic acquisitions for angiography and are particularly well suited to peripheral MR angiographic applications.
- Balanced steady-state free precession (SSFP) without arterial spin labeling (ASL) can be performed with ECG gating for thoracic aortic MR angiography and with both ECG gating and navigator-gated free breathing for whole-heart coronary artery MR angiography.
- ASL with either balanced SSFP or partial-Fourier FSE relies on spin tagging to generate image contrast and can be used in a variety of applications, including pulmonary, carotid, renal, and distal peripheral MR angiography.

Summary of General Principles of Vascular MR Imaging

Prior to discussing nonenhanced MR angiographic methods, some relevant underlying principles governing angiographic imaging are reviewed.

Arterial and Venous Flow Patterns

Peak systolic flow in arterial vessels typically occurs 150–200 msec following the R wave of ECG tracings. The delay between peak systolic flow and ventricular contraction lengthens as the pulse

Published online

10.1148/radiol.2481071497

Radiology 2008; 248:20–43

Abbreviations:

ASL = arterial spin labeling
 ECG = electrocardiography
 FSE = fast spin echo
 MIP = maximum intensity projection
 SSFP = steady-state free precession
 3D = three-dimensional
 TOF = time of flight
 2D = two-dimensional

wave moves distally toward the extremities because of the compliance of the arterial structures (24,25). While peak systolic velocity ranges from 70 to 100 cm/sec in the abdominal aorta, it is usually much lower in the peripheral vessels, ranging from 30 to 50 cm/sec in the femoral artery compared with 10–20 cm/sec in the dorsalis pedis (26). The pulse waveform varies across the vascular system. The reversal of arterial flow due to diastolic filling of the coronary arteries can be seen throughout the thoracic aorta. For other arteries, the appearance of the velocity waveform of an artery depends on vessel wall compliance and whether the artery feeds a high- or low-resistance structure. For example, lower extremity arteries supply high-resistance muscle beds, resulting in the triphasic appearance of their velocity waveforms. The triphasic appearance is dampened in diabetic patients with calcified, attenuated, or stenotic vessels (25,27). In contrast, vessels such as the internal carotid artery and renal artery that supply low-resistance vascular beds have a high forward flow during diastole. Venous flow does not demonstrate pulsatility. Rather, its slow flow varies with respiration as negative intrathoracic pressure accelerates venous return to the chest.

T1 and T2 of Blood Compared with Other Tissues

Arterial and venous blood have relatively long T1 relaxation times in vivo. The values depend on the oxygenation status of the blood. For arterial blood, T1 times of 1200 msec are typically cited at 1.5 T (28), although exact values depend on hematocrit level, oxygenation, and temperature. Venous T1 values do not differ substantially from arterial T1 times. T1 values generally increase at higher magnetic field strengths. For example, the T1 of brain parenchyma increases by 25%–40% at 3 T (29), while on average, T1 relaxation times are 21% longer for kidney cortex, liver, and spleen (30). T2 relaxation times depend strongly on oxygenation. Arterial blood T2 relaxation times at 1.5 T are typically around 250 msec (31,32), while venous blood T2

values are shorter, at about 30 msec for an oxygen saturation of 30% (32). Relevant to peripheral MR angiographic imaging techniques with T2 weighting, it has been observed that deep veins have longer T2 times compared with superficial veins (33,34).

Key Characteristics and Imaging Requirements across MR Angiographic Applications

Of the angiographic applications, carotid, peripheral, renal, and coronary MR angiography exemplify the different challenges of vascular imaging. For carotid MR angiography, the small size of the vessels combined with the clinical need to differentiate between fine grades of stenosis demands high spatial resolution on the order of 1 mm or less. At the same time, for contrast-enhanced methods, rapid venous enhancement limits the window for venous-free carotid MR angiography.

For peripheral MR angiography, the extensive anatomic coverage desired—typically at least 80 cm to as much as 140 cm from the renal arteries to the toes—requires efficient imaging techniques so that multiple stations can be imaged during a short examination period. Spatial resolution is particularly important for visualizing small vessels. Patency of pedal arteries may be the determining factor for revascularization versus amputation in patients with limb-threatening ischemia (35,36). The flow patterns in the peripheral vessels can also be complex. Both differences in atherosclerotic disease and hyperemia associated with foot ulcers can cause different rates of enhancement for two extremities. Retrograde filling of proximally occluded vessels can result in delayed cephalad flow patterns of some arterial structures. In these settings, dynamic imaging that provides temporal information about arterial flow can be clinically valuable (37). Additionally, the close proximity of paired veins alongside peripheral arteries can make interpretation of MR angiographic findings a challenge unless venous signal is suppressed.

For the renal arteries, imaging with certain nonenhanced techniques can be

particularly challenging because of the different orientations of the renal arteries and their branches relative to the aorta and renal artery motion with respiration. Similar challenges face applications of MR angiography to the thoracic aorta and subclavian arteries in the evaluation of thoracic outlet syndrome or in upper-extremity MR angiography. Spatial resolution demands for renal MR angiography are also high, particularly for evaluation of possible fibromuscular dysplasia or other branch-vessel disease. Like for carotid arteries, rapid venous enhancement also restricts the window of acquisition for high-quality, arterially selective, contrast-enhanced MR angiography.

Figure 1

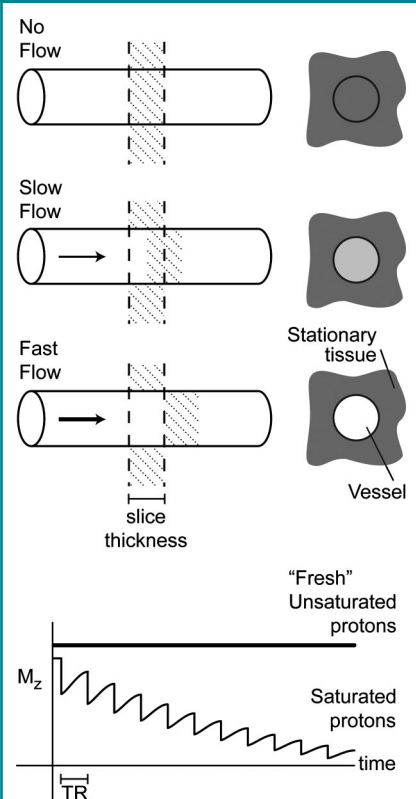


Figure 1: Schematic of TOF MR angiographic principles. Stationary protons exposed to repeated radiofrequency excitation pulses lose signal because of saturation. Arrival of fresh protons results in increased signal intensity, particularly when there is complete replacement of protons in the section between each excitation pulse. M_z = magnetization, TR = repetition time.

Finally, for the coronary arteries, minimizing motion artifacts requires acquisition during a limited period of the cardiac and respiratory cycles. High image contrast for the visibility of the coronary arteries requires suppression of

myocardial tissue and coronary venous signal. Moreover, high spatial resolution is critical to resolving clinically important differences between mild, moderate, and severe stenoses.

TOF MR Angiographic Techniques

The most commonly used nonenhanced MR angiographic technique has been TOF imaging (38–42), developed in the late 1980s. TOF angiography relies on the differences in exposure to radiofrequency excitation between in-plane or in-slab stationary protons and the blood protons flowing into the section or slab (Fig 1). Stationary protons in the imaging section become relatively saturated with repeated excitation pulses and produce low signal intensity. Inflowing blood protons in arteries and veins have not experienced the excitation pulses, are not saturated, and therefore generate high signal intensity. For selective imaging of arteries, saturation bands are applied on the venous side of imaging sections to null signal from the venous flow. Flow-compensation gradients, consisting of additional positive and negative-lobed gradients applied in one or more directions, reduce flow-related dephasing.

The contrast between inflowing arteries and background tissue in TOF MR angiography depends on certain imaging parameters. Longer repetition times allow for inflow of arterial protons, but at the expense of increased imaging times. With thinner sections, shorter repetition times can be used, although the gain in time with shorter repetition time is offset by the need to image more sections for the same anatomic coverage; typically repetition times for 2D imaging range from 25 to 50 msec. The higher the flip angle the greater the suppression of background tissue and the greater the signal from the fully magnetized inflowing arterial protons, provided flow is sufficiently fast for all spins to be completely replaced in a section with each excitation. Flip angles can vary from 25° to 60°, depending on the application.

Acquisitions can be performed by using 2D or 3D methods, depending on the spatial resolution and the extent of the vascular territory to be imaged. Today, the most common clinical application of TOF angiography is the examination of intracranial vessels (38,39), for which 3D methods are preferable to achieve high-spatial-resolution isotropic imaging (Fig 2). In contrast, for peripheral MR angiography, the extensive anatomic coverage desired makes 3D imaging impractical. In clinical practice, 2D TOF angiography is still used for evaluation of tibial and pedal arteries and has been shown to be as accurate as conventional angiography for the diagnosis of stenosis and occlusion in multicenter studies (43–46) (Fig 3).

Limitations of TOF imaging include the saturation of protons in vessels within the imaging section or slab, particularly in 3D imaging, in general, or in 2D imaging, where flow lies within the plane of imaging. Improvements to enhance inflow effects in intracranial 3D TOF include tilted optimized nonsaturating excitation, or TONE (47), which uses progressively increasing flip angles through the slab to compensate for saturation of blood flowing in the slab (Fig 2), and multiple overlapping thin slab acquisition, or MOTSA, which repre-

Figure 2



Figure 2: Intracranial 3D TOF imaging in a 35-year-old man with a history of headaches. Maximum intensity projection (MIP) demonstrates a pial arteriovenous malformation. Imaging was performed by using magnetization transfer and tilt optimized nonsaturated excitation to improve sensitivity to flow. (Image courtesy of Dr E. Knopp, New York University Medical Center.)

Figure 3

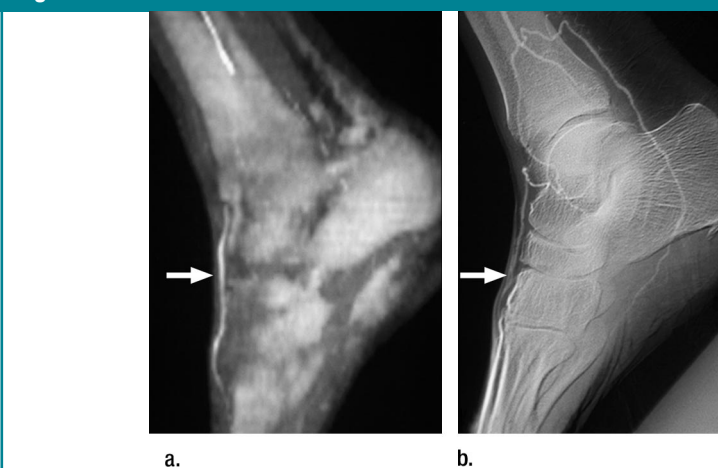


Figure 3: (a) Two-dimensional TOF peripheral MR angiography compared with (b) conventional angiography in a patient with peripheral vascular disease. (a) Sagittal MIP demonstrates patent, reconstituted dorsalis pedis (arrow) and correlates well with (b) the lateral view (arrow). Because a is an MIP, overlapping tissues obscure visualization of the posterior tibial and lateral plantar arteries. On source MR angiograms, both vessels are well seen, comparable to digital subtraction angiograms.

sents a hybrid of 2D and 3D methods (48,49). Application of magnetization transfer pulses improves depiction of intracranial vessels by further suppressing the brain parenchyma signal (47, 50,51) on the basis of differences in T2 relaxation times between free unbound water protons (blood) and protons bound to macromolecules (brain). It should also be noted that with TOF methods, the focus is on flow-dependent luminal imaging. Visualization of the vessel wall is limited, as compared, for example, to gated FSE images.

In the lower extremities, where flow varies with the cardiac cycle, image contrast on TOF MR angiograms can be enhanced by systolic gating. Limitations of 2D imaging of the lower extremities include saturation of in-plane flow, such as at the origin of the anterior tibial arteries on transverse images, which causes pseudostenosis on MR angiograms (Fig 4). Typically, 2D TOF imaging for applications such as carotid and peripheral angiography is performed by using traveling saturation bands to ensure venous nulling. In the extremities, implementation with a caudal saturation band precludes visualization of vessels that may be filled in a retrograde manner (Fig 5). More generally, with 2D TOF imaging, sections must be positioned perpendicular to the direction of flow, which can be challenging in imaging the thoracic aorta or the renal arteries. In most cases, 2D TOF imaging of the extremities has been supplanted by contrast-enhanced imaging for its greater speed, anatomic coverage, and time-resolved capabilities (37).

Phase-Contrast MR Angiographic Techniques

Phase-contrast MR angiography uses pairs of bipolar or flow-compensated and uncompensated gradient pulses to generate flow-sensitive phase images (9,11,12,52). With phase-contrast MR imaging, phase data are used to reconstruct either velocity-encoded flow-quantification images or MR angiographic images. For phase-contrast MR angiography, voxel signal intensity

Figure 4

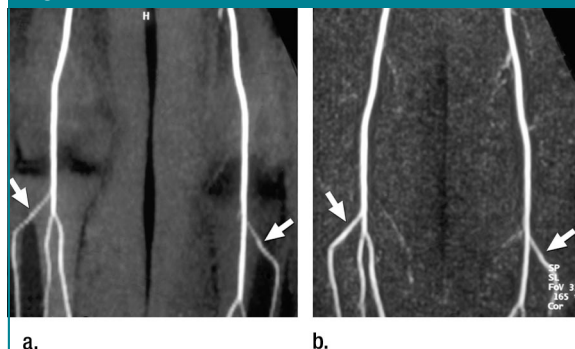


Figure 4: In-plane saturation in anterior tibial artery mimics stenosis at 2D TOF acquisitions in a healthy volunteer. Bilateral proximal anterior tibial artery narrowing (arrows) seen on (a) 2D TOF image is not seen on (b) gadolinium-enhanced MR angiogram.

(SI) reflects the absolute velocity of voxels (v) and is calculated as:

$$SI = \sqrt{v_x^2 + v_y^2 + v_z^2}.$$

So, by definition, signal intensity is always positive, independent of the direction of flow. To produce MR angiographic images with flow sensitivity in three directions, acquisitions need to be repeated four times: one with flow uncompensated and three with different flow-compensation directions (53). Phase-contrast MR angiography has the advantage of high sensitivity to turbulent flow that can be associated with vascular stenoses and inherently low background signal (Fig 6).

For flow quantification, velocity-encoded images are generated by using the net phase shift, computed by subtracting the phase shifts generated by the two (flow-encoded and flow-compensated) acquisitions. On velocity-encoded images, the signal intensity on the image is directly proportional to the phase shift accumulated, where phase shift ranges from 180° to -180° . Positive phase shifts appear with increasing brightness, while negative phase shifts have increasing darkness. The maximum velocity measurable that corresponds to a phase shift of 180° is a user-defined parameter, referred to as encoding velocity, or V_{enc} . For flow quantification applications, where velocities exceed the V_{enc} , velocity aliasing will occur. Phase-contrast MR angiography is more tolerant to mild velocity aliasing because of the way in which the voxel signal intensities are calculated.

In the late 1990s, phase-contrast MR angiography demonstrated great promise

Figure 5

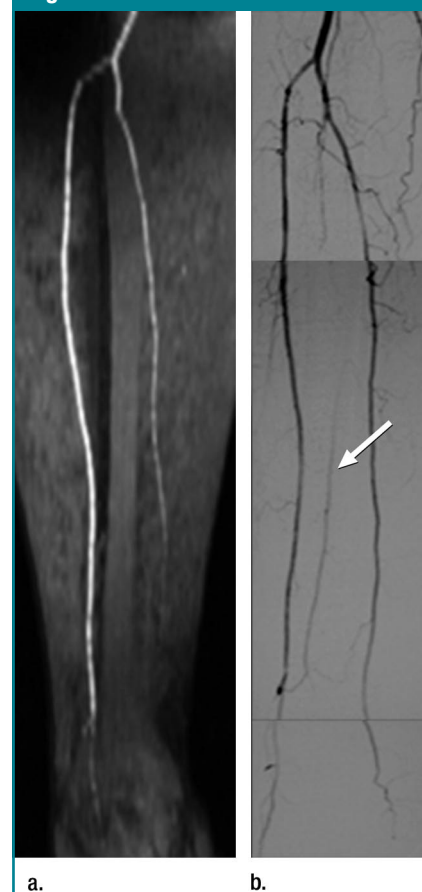


Figure 5: Retrograde filling of right peroneal artery (arrow) on (b) coronal conventional angiogram is not detected on (a) coronal MIP from 2D TOF MR angiography because with the TOF method, a traveling distal saturation band used to suppress venous signal also inadvertently suppressed the retrograde filling peroneal artery. (Reproduced, with permission, from reference 37.)

in a wide range of applications, including renal MR angiography (55–61), peripheral MR angiography (53,62), and portal venography (63). For example, coronal

2D phase-contrast MR angiographic methods for three-station evaluation of the lower extremities—aortic bifurcation to tibioperoneal trunk—have been used with an 80-mm-thick section, 3D flow-encoding with V_{enc} of 30 cm/sec in the iliac arteries and of 20 cm/sec in the femoral and popliteal arteries, and two signals acquired, which resulted in imaging times of 4–7 minutes per station, or an overall acquisition time of 20–30 minutes. In a study of 115 patients with 253 atherosclerotic lesions, the sensitivity of phase-contrast MR angiography with this protocol was 95%, specificity was 90%, positive predictive value was 90%, and negative predictive value was 96% (53,62).

Although recent technical developments using undersampling methods to shorten acquisition times promise to make phase-contrast MR angiography more clinically practical (64,65), the relatively long acquisition times of most currently available phase-contrast MR angiographic sequences preclude their

routine use except for specific applications. Low-spatial-resolution phase-contrast MR angiography is commonly used as a scout sequence for extracranial carotid MR angiography. As a supplemental sequence to diffusion- and perfusion-weighted imaging, Liu et al (66) demonstrated the utility of a 2D phase-contrast MR angiographic acquisition for the evaluation of stroke prognosis. Prince et al (61) have advocated the supplemental use of 3D phase-contrast MR angiography to distinguish between mild and moderate or severe renal artery stenosis (Fig 6). Iseda et al (67) used 3D phase-contrast MR angiography similarly to help characterize physiologically significant carotid artery stenoses. As a supplement to MR angiographic methods, flow quantification with 2D phase-contrast imaging, an application distinct from MR angiography, is potentially valuable for estimating flow and pressure gradients across stenoses in the carotid arteries (68), peripheral arteries (69,70), and renal arteries (71–77), as well as supplementing MR angio-



Figure 6: (a) Axial 3D phase-contrast image depicts bright signal in the initial part of the left renal artery stenosis, where flow is accelerating, and there is complete signal dropout beginning at the most severe part of the stenosis and extending for 1 cm distally (arrow). (b, c) Corresponding 3D gadolinium-enhanced MR angiograms in (b) coronal and (c) transverse views show a widely patent aorto-bi-iliac graft and severe left renal artery stenosis (arrow). The signal dropout from spin dephasing in a indicates there is a pressure gradient across the stenosis. (Modified, with permission, from reference 54.)

Figure 7

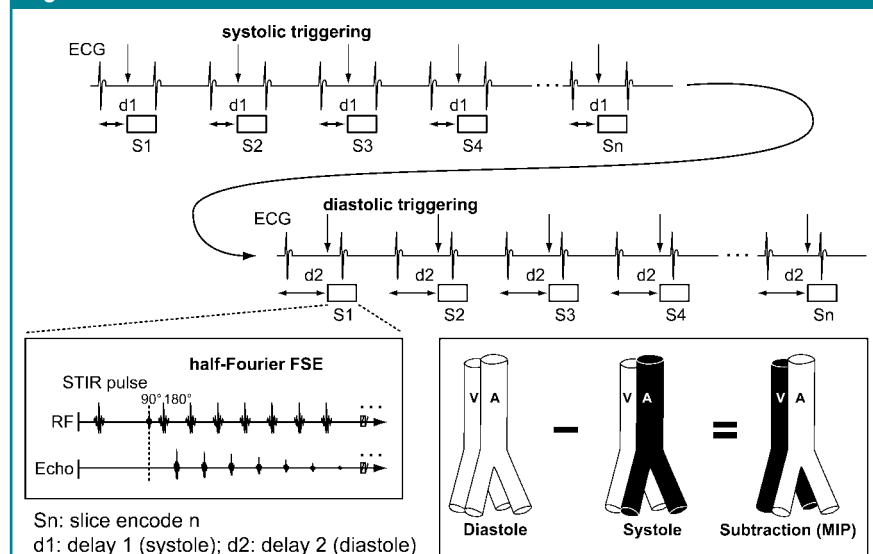
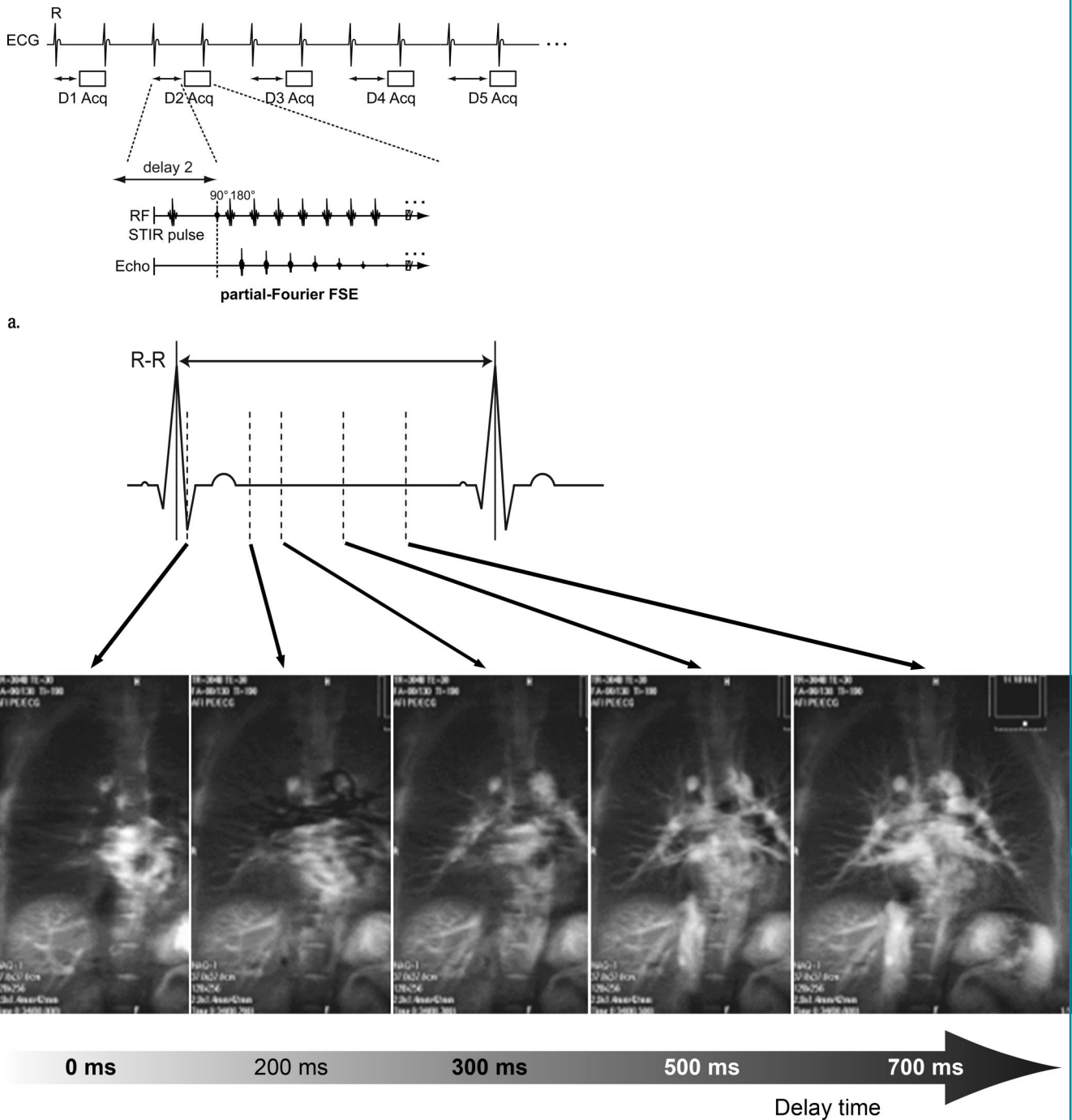


Figure 7: Three-dimensional partial-Fourier FSE imaging with systolic and diastolic acquisition. Each section (S_1, S_2, \dots, S_n) is imaged in one single-shot acquisition. One trigger delay (d_1) is timed for systole for one 3D acquisition, while a second delay (d_2) is timed for diastole. Acquisitions are performed every other or every third heartbeat. A short tau inversion-recovery (STIR) pulse can be used for improved fat suppression. To generate a bright-blood angiogram, systolic images (where arterial flow appears dark) are subtracted from diastolic images. A = arteries, RF = radiofrequency, V = veins. (Modified, with permission, from reference 85.)

Figure 8



b. **Figure 8:** ECG preparatory scan to determine appropriate ECG delay time for systolic and diastolic triggering times; scan is performed prior to 3D acquisition. **(a)** Sequence diagram shows repeated 2D single-shot partial-Fourier acquisitions (*Acq*), each acquired with progressively longer trigger delay times (*D1, D2, ... D5*) following the R-wave of the ECG tracing. **(b)** Single-shot images from selected delay times show typical results of ECG preparatory scan. For pulmonary angiography in this example, a systolic trigger of around 200 msec would result in desired flow void, and diastolic triggering gives bright-blood images at a delay of 700 msec. *RF* = radio-frequency, *STIR* = short tau inversion recovery. (Modified, with permission, from reference 85.)

graphic evaluation such as in thoracic dissection (78) and coarctation (79), subclavian steal syndrome, intracranial ischemia (80), central pulmonary arteries (81), and intracranial vascular malformations (82).

Figure 9

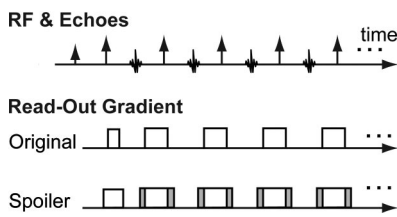


Figure 9: Spoiler gradients, representing extended applications of gradients to dephase magnetization, in the readout direction. *Original* = readout gradient in conventional partial-Fourier FSE implementation. *Spoiler* = readout gradient with additional spoiler gradients to improve sensitivity to slow flow in the readout direction in 3D ECG-gated partial-Fourier FSE MR angiography. If the signal difference between diastolic and systolic flow is small, strong spoiler gradients (larger gray areas) are applied. RF = radiofrequency. (Modified, with permission, from reference 86.)

ECG-gated 3D Partial-Fourier FSE Sequence

One of the two newer methods that is demonstrating promise for clinical use as a nonenhanced MR angiography technique was first described in principle in the 1980s by Wedeen et al (83) and Meuli et al (84) using an ECG-gated spin-echo sequence. Recent improvements in the approach, including use of single-shot partial-Fourier FSE sequences (also referred to as single-shot FSE, half-Fourier rapid acquisition with relaxation enhancement, or fast asymmetric FSE) have shortened the acquisition times and have made this method clinically feasible on modern MR systems, with resulting early commercial availability on some systems (85,86). In this section, we introduce the reader to the principles of this up-and-coming technique in some detail, discuss applications, and consider its limitations.

Principles of the Technique

This nonenhanced MR angiographic technique relies on an ECG-gated 3D partial-Fourier FSE sequence, which is triggered for systolic and diastolic acquisitions.

The method relies on loss of signal, or flow void, as a result of fast arterial flow during systole. In contrast, during diastole, the slow flow in arteries causes them to have high signal intensity on T2-weighted images. Because of its relatively slow flow, venous blood is bright during both systole and diastole. Bright-blood MR angiography is then achieved by subtracting systolic from diastolic images (Fig 7). Interestingly, a similar nonenhanced approach for MR angiography can also be achieved with gradient-echo imaging by using ECG gating and uncompensated gradients to accentuate flow voids during systole and flow-compensated gradients to increase signal in arteries during diastole (87). However, longer acquisition times for comparable spatial resolution limit application of this method compared with FSE approaches.

Synchronization with the cardiac cycle can be achieved with ECG gating or peripheral pulse wave gating. To keep acquisition times reasonable, the 3D sequence is typically implemented with each partition acquired in a single shot (Fig 7). To allow sufficient T1 recovery, the repetition time for these gated acquisitions is typically every two to three heartbeats (R-R intervals). The triggering time is the same for all partitions. The acquisition time for each 3D image depends on the number of partitions or sections and is typically 90 seconds to 3 minutes. Performance of the systolic and diastolic 3D acquisitions continuously and without interruption minimizes misregistration and motion artifacts on subtracted images for an overall acquisition times of about 3–6 minutes. Concepts essential to successful bright-blood MR angiographic images with this technique are discussed next (85,86).

First, a T2 blurring effect in the phase-encoding direction at FSE-type sequences is related to the sampling of multiple echoes at different echo times (88). If the vessels are oriented perpendicular to the phase-encoding direction, as in peripheral MR angiography, the T2-blurring effect results in undesirable vessel blurring artifacts.

Second, to maximize differences between systolic and diastolic images, re-

Figure 10

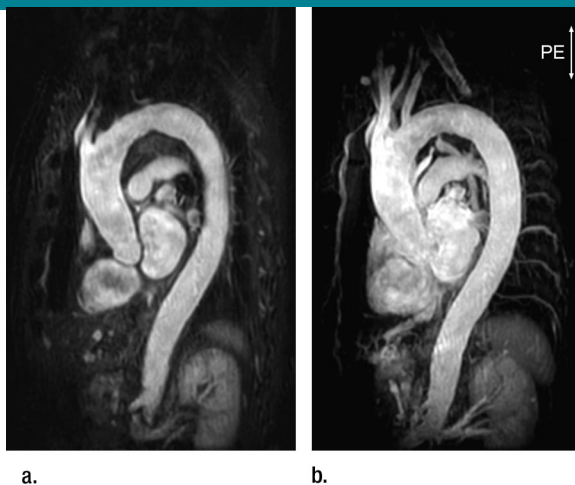


Figure 10: Nonenhanced MR angiography of the aorta in 32-year-old female volunteer with 3D ECG-gated partial-Fourier FSE (repetition time/effective echo time msec, four R-R intervals/30; 180° flip angle). (a) Source image and (b) MIP of diastolically triggered images obtained by using a trigger delay of 600 msec and echo train length of 67 in two separate shots, which resulted in 335-msec acquisition window per shot. Eight 3-mm sections were acquired and interpolated to 16 1.5-mm sections. Phase-encoding directions were craniocaudal and anteroposterior. Total scan time was about 3 minutes with an intermittent breathhold technique. (Image courtesy of J. Urata, Saiseikai Kumamoto Hospital, Japan.)

duce T2 blurring, and minimize motion-related artifacts, the total data sampling duration during each heartbeat should be as short as possible. If each partition is acquired in a single shot, a short interecho train spacing is desirable. For example, if the echo train length is 70 with parallel imaging, an interecho train spacing of 5 msec results in an acquisition time of 350 msec per heartbeat. Although this time exceeds the typical duration of systolic flow, the careful determination of a triggering time for peak systolic flow, combined with use of centric reordering, can help to preserve the desired flow voids with a single-shot FSE sequence. Alternatively, data for each partition can be collected in two shots, which results in sharper images by reducing the data sampling window time. However, the scan time will double that of a single-shot method. Application of parallel imaging has allowed shorter data sampling periods, with advantages of more precise imaging during systole and reduced T2 blurring.

Third, with a rectilinear k-space filling, centric ordering results in intrinsically less flow dephasing in the phase-encoding direction compared with the readout direction (89). As discussed in more detail below, depending on the application, the orientation of the readout or frequency-encoding direction relative to the vessels of interest can be selected to optimize arterial signal. For the relatively slower moving protons in the peripheral arteries, the readout direction can be oriented in the direction of flow and flow-spoiling gradient pulses can be applied in the readout direction to increase the flow-dephasing effect during systole. Flow-spoiling gradient pulses accentuate the differences in signal between systolic and diastolic phases without affecting slower flowing venous blood and the stationary background signals.

Last, additional prepulses can be used in conjunction with the 3D partial-Fourier FSE method to achieve different types of image contrast. For example, use of a short tau inversion-recovery method can be used to achieve fat-suppressed images (85,86).

Before performance of systolic and diastolic 3D ECG-gated partial-Fourier

Figure 11

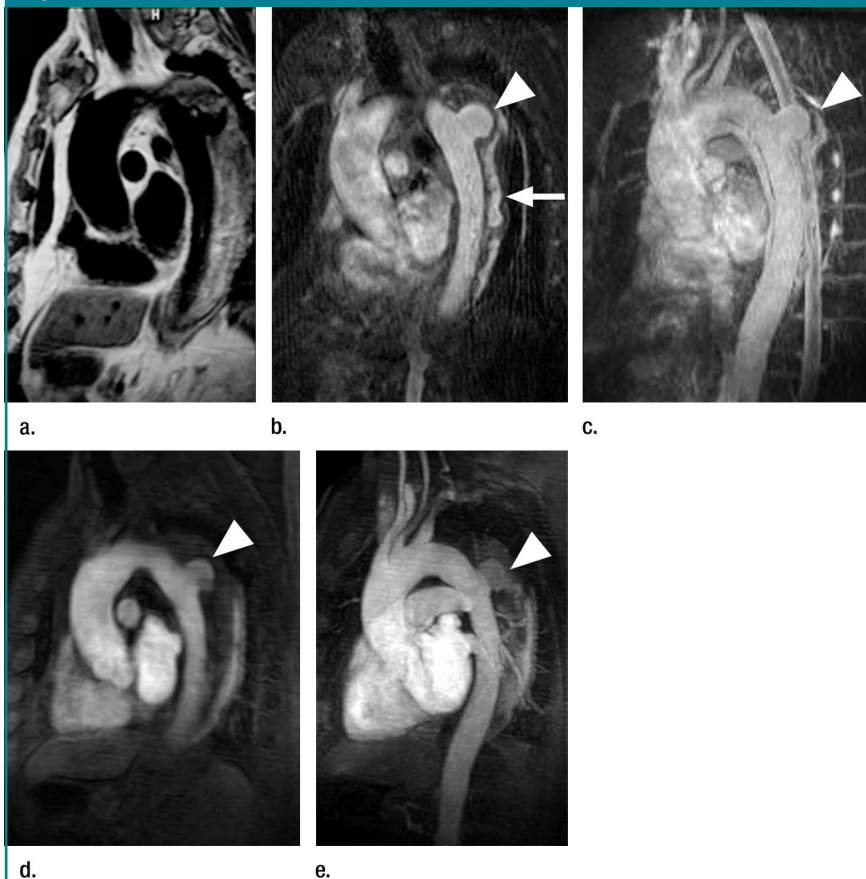


Figure 11: Nonenhanced and contrast material–enhanced MR angiography in 58-year-old man with type B aortic dissection. **(a)** Conventional nonenhanced black-blood ECG-triggered FSE image (three R-R intervals/80, 180° flip angle) with a double inversion recovery FSE sequence (inversion time, 550 msec), **(b)** source image, and **(c)** MIP image from nonenhanced 3D ECG-gated FSE (four R-R intervals/30, 180° flip angle); and **(d)** source image and **(e)** MIP image from contrast-enhanced 3D MR angiography show a thrombosed false lumen and an ulcer-like projection (arrowhead). Areas of high signal intensity are observed in the false lumen in **(b)** (arrow), suggesting stagnant fluid collection not communicating with the true lumen. With nonenhanced methods, mural abnormality is not well depicted on subtracted images; source images must be viewed to evaluate the vessel wall. (Modified, with permission, from reference 21.) (Image **a** courtesy of J. Urata, Saiseikai Kumamoto Hospital, Japan.)

FSE acquisitions, one or two additional preparatory steps can be helpful. First, an “ECG-prep scan” that produces 2D images at incremental triggering times of arbitrary steps can be used to find the trigger delay for systole, when arteries are black blood (flow voids), and diastole, when arteries are bright (85) (Fig 8). A second 2D preparatory scan can determine the amount of flow-spoiling gradient pulses that cause the best selective dephasing of the arteries of interest, particularly in slow-flowing arteries. The operator uses these pre-

paratory scans to define parameters for the 3D acquisition (86) (Fig 9).

Applications of 3D ECG-gated FSE

Specific aspects of the implementation of 3D ECG-gated FSE images vary with the application. Imaging of the thoracic aorta and the peripheral arteries are considered next. Application of a partial-Fourier FSE technique for carotid MR angiography can be challenging because venous signal can appear on subtracted images due to the relatively fast flow of the jugular veins. For renal MR angiography, the

orthogonal directions of flow in the aorta and renal arteries present challenges for the FSE method. Therefore, for nonenhanced carotid and renal MR angio-

graphic acquisitions, balanced SSFP with ASL may be preferable (see below).

Thoracic aorta.—The fast-flowing blood in the thoracic aorta consistently

produces a flow void (black blood) during systole and a high signal (bright blood) during diastole (85). For the thoracic aorta, the phase-encoding direction should be oriented parallel to the direction of flow (craniocaudal) with the application of presaturation bands superior and inferior to avoid wraparound artifacts. Also, since venous enhancement is not seriously detrimental to image quality, these acquisitions can be performed with a single diastolic acquisition.

Typical nonenhanced MR images of the aortic arch by using gated 3D FSE methods are presented in Figure 10. In a prospective study of 75 patients referred for thoracic aortic MR angiography (34 with dissection, 27 with aneurysm, four with arterial occlusion, 10 with surgical bypass), image quality of the nonenhanced images was excellent in 45, satisfactory in 25, and poor in five patients. In all 34 cases of dissection, the intimal flap was consistently visualized (21). Figure 11 compares three methods: black-blood partial-Fourier FSE, nonenhanced 3D ECG-gated FSE, and gadolinium-enhanced MR angiography in a patient with a type B aortic dissection.

Peripheral MR angiography with flow spoiling and flow compensation.—Unlike thoracic aortic applications, the frequency encoding or readout gradient for peripheral MR angiography is oriented in the direction of flow to improve systolic flow spoiling. Additional readout gradient pulses can be added to provide flow spoiling or flow compensation as needed for optimal systolic flow void imaging (86).

Figure 12 shows typical diastolic and systolic-triggered images and the resulting arteriogram generated by subtraction of systolic images from diastolic images. In this case, flow spoiling of -10% (or partial-flow compensation) was used in the iliac to thigh region to compensate for the fast flow of blood. Vessels with slower flowing blood such as the calf (Figs 13, 14), pedal (Fig 15), and hand (Fig 16) arteries are usually imaged with this approach by using stronger flow-spoiling pulses to differen-

Figure 12

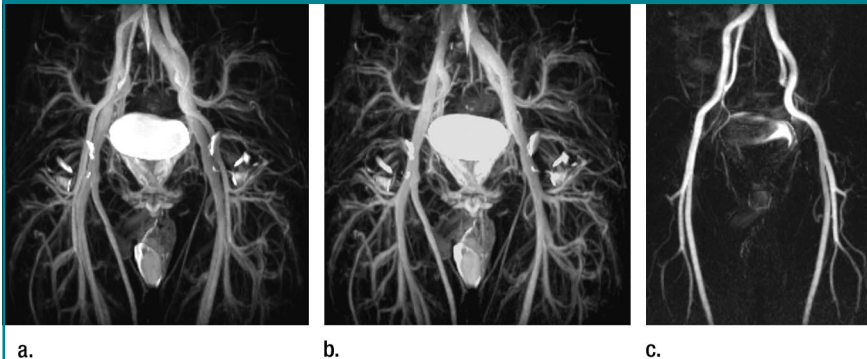


Figure 12: Nonenhanced MR angiography of the pelvis and thighs in a 34-year-old healthy male volunteer with 3D ECG-gated partial-Fourier FSE. (a) Diastolic and (b) systolic-triggered images are subtracted to produce (c) MR angiogram (MIP). Flow spoiling of -10% (or partial-flow compensation) was used in the readout (craniocaudal) direction to compensate for the fast flow of blood.

Figure 13

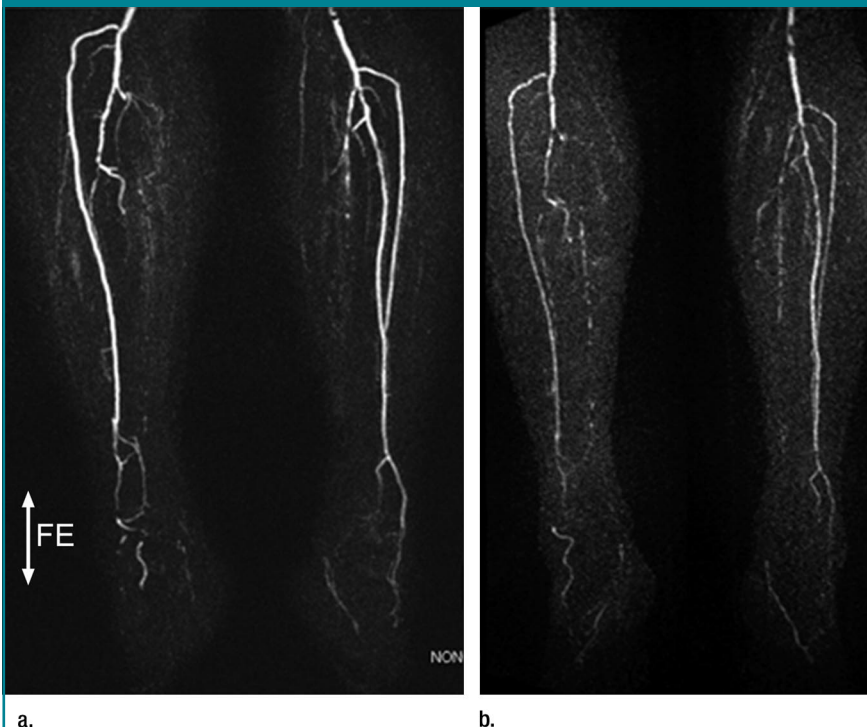


Figure 13: Peripheral MR angiography in a patient with claudication. (a) Nonenhanced 3D ECG-gated partial-Fourier FSE acquisition and (b) gadolinium-enhanced MR angiogram with a time-resolved approach to achieve optimal arterial enhancement. Both images show bilateral severe disease of the calf arteries. Frequency-encoding (FE) direction is craniocaudal. (Image courtesy of R. Lim, New York University Medical Center.)

tiate systolic arterial signal from diastolic signal.

To date, of the three studies (90–92) evaluating flow-spoiled ECG-gated 3D FSE for peripheral MR angiography in clinical subjects, two have been published only in abstract form. Although preliminary, these results reflect a range of experiences with the 3D FSE method. In their initial clinical study in 2002, Urata et al (90) found that the ECG-gated FSE method was comparable to gadolinium-enhanced MR angiography in 24 of 44 regions, while 15 were inferior and five were superior when tested in a total of 56 regions (18 iliac, 20 femoral, and 18 calf area) in 26 patients diagnosed to have or suspected of having arterial occlusive disease. To avoid overestimation of stenoses, the investigators in this study (90) suggested that diastolic images, which depict both arteries and veins, always be evaluated in addition to subtracted MIP images. Nakamura et al (92) used a similar strategy in their study of 13 patients with 56 diseased segments and compared MR angiography with 16-detector computed tomographic (CT) angiography; they found that the MR method resulted in a sensitivity of 94%, a specificity of 94%, and an accuracy of 94% for the detection of 50% or greater stenosis (Fig 17).

In a separate study, Lim et al (91) compared the nonenhanced method in the distal station (calf and pedal arteries) with conventional bolus-chase imaging and 3D time-resolved contrast-enhanced MR imaging in 36 patients, where the reference standard was a combined consensus interpretation of all three sequences. When all subjects were studied, the non-contrast technique demonstrated accuracy of 79.4% (1083 of 1364), sensitivity of 85.4% (437 of 512), and specificity of 75.8% (646 of 852), with a high negative predictive value of 92.3% (646 of 700). Serious artifacts lead to poor diagnostic confidence in 17 patients (47.2%). Among patients with satisfactory diagnostic confidence, accuracy, sensitivity, and negative predictive value were 92.2% (661 of 717), 92.4% (158 of 171), and 97.5 (503 of 516), respectively (Figs 13, 14). One limitation of the study was that only the subtracted MIP images were evaluated.

Figure 14

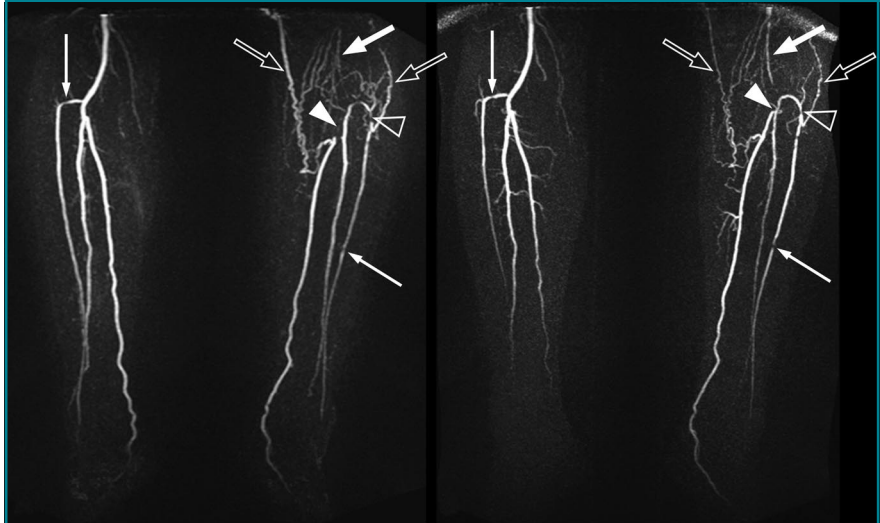


Figure 14: MIP from calf MR angiography in 79-year-old man with left leg claudication. Left: ECG-gated FSE image (two R-R intervals/49, 101° flip angle) shows severely diseased left popliteal artery (solid arrow) with distal occlusion; proximal occlusion of trifurcation vessels, including the posterior tibial artery (solid arrowhead); and severe stenosis of proximal anterior tibial artery (open arrowhead). Collateral supply to both anterior and posterior tibial arteries (open arrows) and clear depiction of focal stenoses of right proximal anterior tibial artery and left mid anterior tibial artery (thin solid arrow) are noted. Right: Gadolinium-enhanced MR angiogram confirms findings. (Image courtesy of R. Lim, New York University Medical Center.)

Figure 15



Figure 15: Digital arterial MIP in a 37-year-old healthy male volunteer. Foot images acquired in a prone position by using a quadrature knee coil. Nonenhanced MR angiogram with 3D ECG-gated partial-Fourier FSE (three R-R intervals/30, 180° flip angle, 192 × 192 matrix interpolated to 384 × 384). For slower flow of the arteries of the feet, stronger flow-spoiling pulses, 35% in this case, are used to differentiate systolic arterial signal from diastolic signal. (Image courtesy of I. Fujita, Saitama City Hospital, Japan.)

Clearly, additional data in patients with peripheral artery disease are needed to evaluate the practical use of this technique in the clinical setting.

Limitations

The ECG-gated 3D FSE method has the advantage of not requiring intravenous contrast material. Disadvantages include the longer scan times compared with those of contrast-enhanced methods. For each acquisition, the nonenhanced method requires 1–3 minutes, compared with the contrast-enhanced 3D gradient-echo sequences that require only 15–25 seconds. As will be discussed in Future Directions, the implementation of parallel imaging will shorten acquisition times and improve image quality. Another limitation of this method is that on subtraction images, vessel wall abnormalities can be missed. Review of source images is necessary to visualize abnormalities such as intramural hematoma and aortic dissections with slow flow.

The most important technical challenge limiting the robustness of the method across patients with varying degrees of disease is imperfect timing of the triggered acquisitions. Inappropriate selection of the systolic trigger delay leads to suboptimal flow voids on systolic images and resulting overestimation of stenosis and underestimation of vessel length on subtracted datasets. This problem is exacerbated by reliance on subtraction images for evaluation of stenosis. Two other technical issues include improving sensitivity to vessels with varying flow patterns, particularly

distal to a stenosis, or in collateral vessels. Additionally, the relatively long sampling window during each cardiac cycle (typically 325 msec per partition without parallel imaging) results in degraded image quality due to motion artifacts and blurring. Higher parallel imaging factors, particularly at higher magnetic field strengths, may help overcome these problems by reducing the number of echoes per partition and consequently reducing vessel blurring by reducing T2-blurring effects and minimizing motion-related artifacts. Finally, patients with arrhyth-

Figure 16

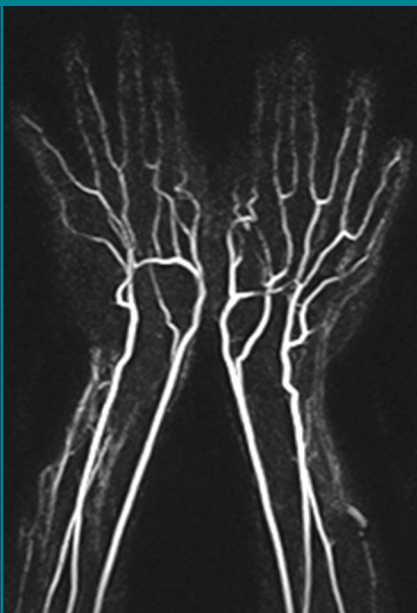
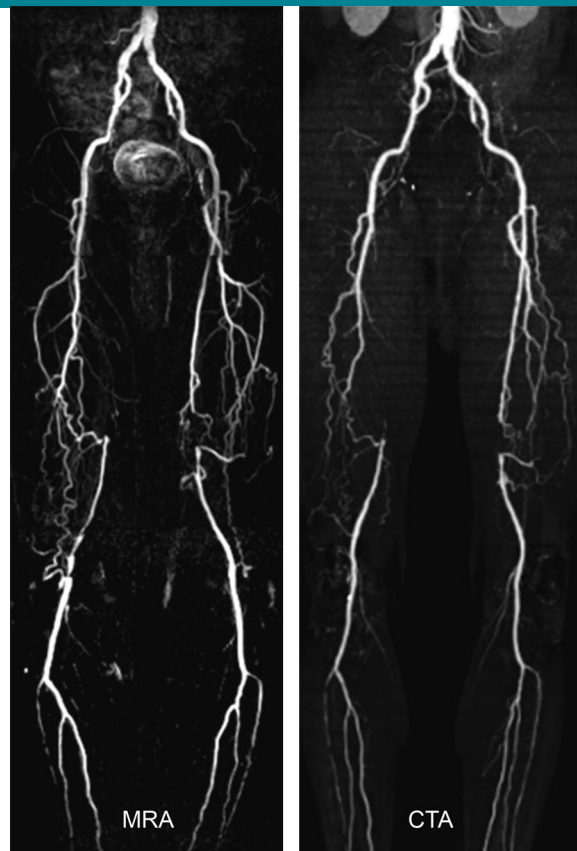


Figure 16: Nonenhanced MR angiogram of the hands and forearms in a healthy volunteer with 3D ECG-gated partial-Fourier FSE. Additional flow spoiling was used to achieve sensitivity to slower flowing arteries in the hand. (Image courtesy of Jian Xu, Siemens and New York University Medical Center.)

Figure 17



a. b.

Figure 17: Comparison of three-station nonenhanced MR angiography with 16-detector CT angiography in a 64-year-old male patient with bilateral atherosclerotic disease. (a) ECG-gated 3D partial-Fourier FSE MR angiogram obtained for three stations by using flow-spoiling pulses of 0, +5%, and +10% in iliac, femoral, and calf regions, respectively. Note the depiction of collateral vessels achieved with parallel imaging and resolution of 256×256 matrix interpolated to 512×512 (three R-R intervals/80, 160° flip angle, parallel factor of two, 4-mm section thickness and 2 mm after interpolation, and 37×37 cm field of view) and (b) contrast-enhanced CT angiogram in the same subject. (Image courtesy of K. Nakamura, Kyoritsu Tobata Hospital, Japan.)

mias, particularly tachyarrhythmias, can be problematic and may also benefit from shorter acquisition windows.

Balanced SSFP without ASL

Principles of Technique

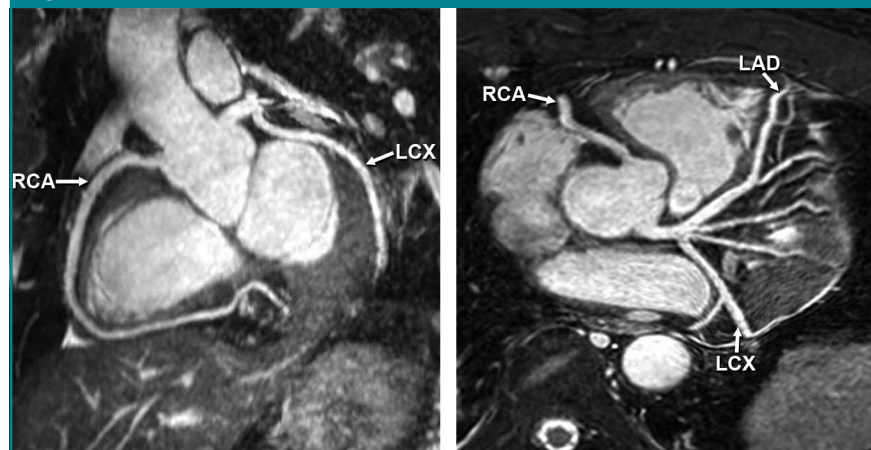
Although initially described by Carr in 1958 (93), balanced SSFP sequences have enjoyed a recent resurgence of interest across a wide range of applications (94). The technique lends itself well to angiographic applications because image contrast is determined by T2/T1 ratios, which produce bright-blood imaging without reliance on inflow. The technique can therefore take advantage of recent advances in hardware that permit short repetition times of less than 3–4 msec and with use of high flip angles can produce high-signal-to-noise ratio MR angiographic images that are suitable for parallel imaging. With balanced SSFP, both the arteries and the veins have high signal intensity, and therefore most MR angiographic applications utilize additional preparatory pulses to selectively enhance arteries (see section on coronary arteries below). Additionally, with renal MR angiographic applications, most methods also rely on saturation bands over kidneys and inferior vena cava to reduce venous signal and fat suppression to null the otherwise high signal of fat in these images (95). Brittain et al (96) have recently shown that at 3 T, the greater sensitivity to oxygenation differences allows for better venous suppression with longer repetition time for SSFP MR angiography.

Two main applications of balanced SSFP without ASL MR angiography have been gaining acceptance—coronary MR angiography and thoracic aortic MR angiography.

Applications

Coronary MR angiography.—Among the most popular applications of balanced SSFP is its use with coronary MR angiography (97). Most commonly, 3D SSFP coronary MR angiographic techniques have been implemented by using thin slabs and breath-hold acquisi-

Figure 18



a.

b.

Figure 18: Reformatted 3D SSFP whole-heart coronary MR angiography (4.6/2.3; 90° flip angle; navigator gated with fat saturation and T2 preparation) in a 42-year-old man with normal coronary arteries. (a) Left anterior oblique whole-heart angiogram with curved multiplanar reformatting clearly depicts the right coronary artery (RCA) and left circumflex (LCX) arteries. (b) Oblique axial whole-heart coronary MR angiogram with curved multiplanar reformatting shows the left main coronary artery, left anterior descending (LAD) artery, proximal RCA, and LCX arteries. (Reproduced, with permission, from reference 101.)

tions (97–100), thin-slab navigator-gated acquisitions (99) and, more recently, whole-heart acquisitions during navigator-gated free breathing (101). To improve coronary artery conspicuity, these sequences are typically implemented by using T2 preparation to suppress myocardial and venous signal (98,102) and fat-suppression pulses. Sakuma et al (101) demonstrated successful completion of MR angiography in 34 of 39 patients, with average imaging times of 13.8 minutes \pm 3.8 (standard deviation). In their experience, the overall sensitivity for detecting significant stenosis was 82% and specificity was 91% (Fig 18). Defining acquisition windows during periods of minimal coronary motion in diastole is critical to the quality of the resulting images, although a recent study (103) suggested that patients with high heart rates may benefit from systolic gating. Sequences can be implemented with Cartesian or radial sampling, and results suggest reduced image artifacts with radial methods (102). The high signal-to-noise ratio of balanced SSFP sequences lends itself well to parallel imaging; a recent study showed feasi-

bility of breath-hold whole-heart coronary MR angiography by using a 32-channel coil with high parallel factors (104). The advantage of these methods is that both the coronary lumen and the vessel wall are visualized. For imaging of the vessel lumen only, ASL has been proposed in conjunction with balanced SSFP for coronary MR angiography (105,106).

Thoracic aortic MR angiography.—Without the necessity for venous or fat suppression, combined with the fast flow of blood in the thoracic aorta, thoracic MR angiography is perfectly suited to balanced SSFP without ASL. When implemented with ECG gating and triggered for diastolic acquisitions, 3D MR angiography can be achieved with respiratory triggering in acquisition times of 5–10 minutes with use of parallel imaging (Fig 19).

Limitations

Balanced SSFP without ASL can be more difficult to implement successfully under certain conditions. The sequence is susceptible to field inhomogeneities, such as at air-tissue interfaces or in the presence of metallic implants. To improve homogeneity, localized shimming

may be necessary, which is typically not required with FSE methods. Additionally, without ASL, these sequences are not specific for arteries or veins. The

addition of spin labeling or other suppression methods such as T2-preparation pulses is necessary to produce venous-free arteriograms.

Figure 19

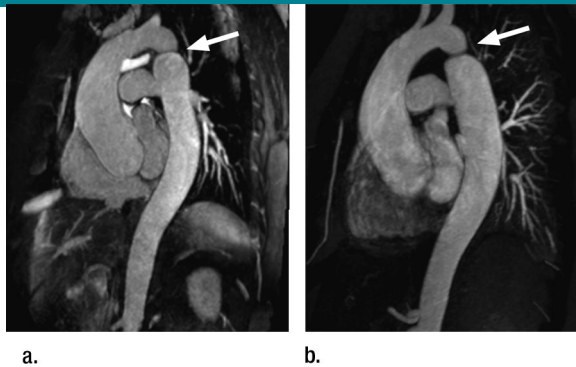


Figure 19: MR angiography of the thoracic aorta in a 37-year-old man with recurrent aortic coarctation (arrow). Thin-section MIPs with (a) cardiac and respiratory-triggered balanced SSFP (259/1.4, 90° flip angle, parallel imaging factor of two, acquisition time of 6.5 minutes) without contrast material and (b) gadolinium-enhanced 3D gradient-echo imaging. (Image courtesy of Monvadi B. Srichai, New York University Medical Center.)

Figure 20

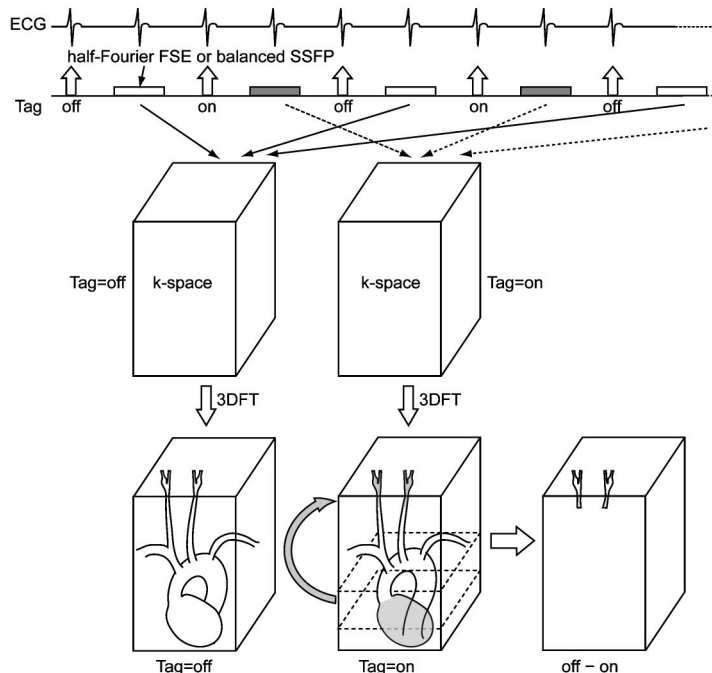


Figure 20: Schematic for ASL-based MR angiography by using tag-on and tag-off images illustrates tagging (dashed box) applied to the chest, over the heart. During the interval, tagged blood moves to the desired imaging region, carotid arteries in this example (curved arrow). Subtracted images produce MR angiograms of carotid arteries, with all background tissue suppressed. This approach can be implemented by using partial-Fourier FSE or balanced SSFP readout techniques. *FT* = Fourier transform.

ASL Imaging

Frequently used for perfusion measurements in the brain and elsewhere, ASL for use with MR angiography can be usefully combined with fast imaging methods such as balanced SSFP and partial-Fourier FSE options. This section describes the principles of ASL for use with MR angiography, considers a range of clinical applications, and concludes with a discussion of technique limitations.

Principles of Technique

In its earliest versions, ASL angiography generally relied on the spin tagging upstream of the arteries of interest by using an inversion pulse to generate image contrast (13–15,107,108). For example, Nishimura et al (13) obtained two images for subtraction, one with an inversion pulse limited to the upstream slab and a second with a nonselective inversion so that upstream tissue was inverted on only one acquisition. After a short fixed time delay after the tagging, the tagged blood flows into the area of interest and the imaging can proceed. The time delay depends on the distance between the tagged and imaged areas and the rate of blood flow. The time delay also affects the signal, since longer delays result in less difference between inverted and noninverted signal because of T1 recovery. If this process is repeated, with alternate acquisition of the tagged and nontagged images and two sets subtracted, the result will be a bright-blood angiogram with no background signal (Fig 20).

Bright-blood ASL imaging can also be produced by using a single acquisition with a combination of a spatially nonselective inversion recovery pulse and a spatially selective tag pulse (109) (Fig 21). The nonselective tag pulse inverts the magnetization of the entire area of imaging. The spatially selective tagging pulse, again applied upstream of the arteries of interest, reverts those protons to full magnetization. The spatially selective tagging pulse can be applied in any orientation to mark specifically the target vessels. A fixed time delay between tagging and imaging serves

two purposes. First, it allows the selectively tagged protons to reach the imaging region. Second, certain background tissues in the imaging region can be selectively suppressed by imaging at their null point. For example, a delay time of about 550 msec can result in nulling of background venous blood signal in the imaging volume.

For regions in which the background tissues have a range of T1 relaxation times, the application of a single inversion time may be insufficient for nulling. In these cases, implementing the tagged and untagged versions enables reliable suppression of background signal with subtraction (Fig 20) (15,108).

Initially implemented by using readout techniques such as segmented turbo fast low-angle shot (turbo FLASH) or echo planar imaging, early results of ASL MR angiography were promising. For example, using a TOF subtraction method with turbo FLASH, Prasad et al (108) demonstrated that renal MR angiography could be performed in 22 seconds by using 10–20-mm-thick sections and no ECG gating. In a pig model, sensitivity for detecting stenosis was 100% compared with that of conventional angiography, with specificity varying from 78% to 94%, depending on the definition for significant stenosis (50% or 70%). More recently, ASL methods have been implemented with two fast imaging methods that have the advantage of higher signal-to-noise ratios compared to those of previous methods: balanced SSFP and partial-Fourier FSE. Published literature on these methods is limited, as will be reviewed below; however, early results are promising.

ASL with balanced SSFP.—The combination of ASL with tagged and untagged balanced SSFP provides bright-blood, venous-free angiographic images with high signal-to-noise ratios (94,110,111). This approach is particularly well suited to evaluation of vessels such as the renal and carotid arteries, because the sequence is flow compensated in all three directions and therefore minimizes sensitivity to flow artifacts.

ASL with partial-Fourier FSE.—As an alternative to balanced SSFP, partial-

Figure 21

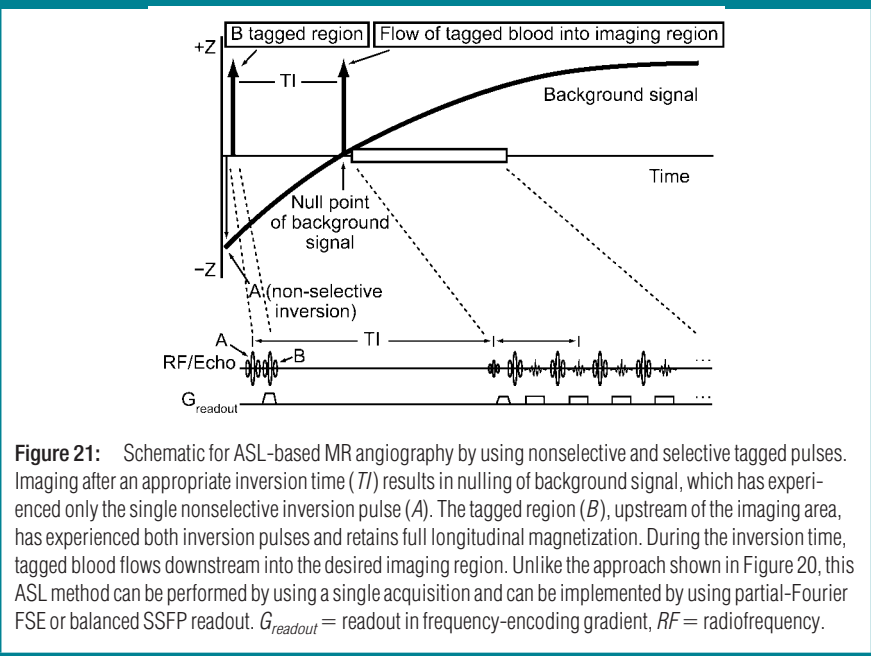


Figure 21: Schematic for ASL-based MR angiography by using nonselective and selective tagged pulses. Imaging after an appropriate inversion time (T_I) results in nulling of background signal, which has experienced only the single nonselective inversion pulse (A). The tagged region (B), upstream of the imaging area, has experienced both inversion pulses and retains full longitudinal magnetization. During the inversion time, tagged blood flows downstream into the desired imaging region. Unlike the approach shown in Figure 20, this ASL method can be performed by using a single acquisition and can be implemented by using partial-Fourier FSE or balanced SSFP readout. $G_{readout}$ = readout in frequency-encoding gradient, RF = radiofrequency.

Figure 22

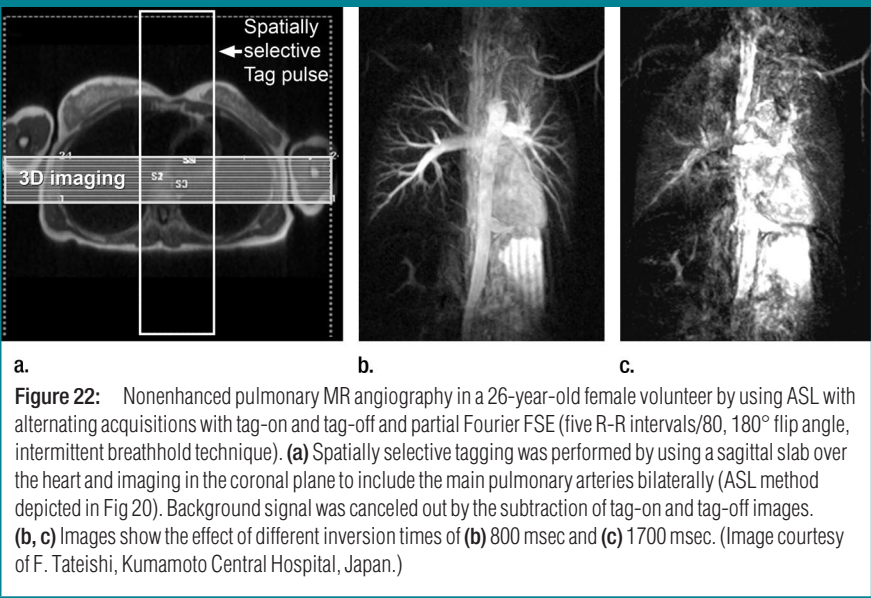


Figure 22: Nonenhanced pulmonary MR angiography in a 26-year-old female volunteer by using ASL with alternating acquisitions with tag-on and tag-off and partial Fourier FSE (five R-R intervals/80, 180° flip angle, intermittent breathhold technique). (a) Spatially selective tagging was performed by using a sagittal slab over the heart and imaging in the coronal plane to include the main pulmonary arteries bilaterally (ASL method depicted in Fig 20). Background signal was canceled out by the subtraction of tag-on and tag-off images. (b, c) Images show the effect of different inversion times of (b) 800 msec and (c) 1700 msec. (Image courtesy of F. Tateishi, Kumamoto Central Hospital, Japan.)

Fourier FSE methods can also be used in conjunction with ASL. The SE-based methods have the advantage of less sensitivity to susceptibility artifacts compared with balanced SSFP. Pulmonary MR angiography with ASL methods therefore benefits from the use of partial-Fourier FSE readout. For all partial-

Fourier FSE methods (see below), improved vascular signal is attained by cardiac triggering for diastolic imaging.

Applications of ASL

Pulmonary MR angiography.—Early results reporting the application of ASL with partial-Fourier FSE to 2D and 3D

pulmonary MR angiography have been reported in abstract form (109,112). The imaging method uses a spatially selective tagging pulse and a nonselective inversion pulse as shown in Figure 22. The tag is applied by using a sagittal band across the heart. During the delay time, that tagged blood from the heart travels into the lungs. Then, the pulmonary arteries are imaged by using a coronal 3D partial-Fourier FSE acquisition. Background signal is canceled out by subtraction of two acquisitions, one with the tag on and a second without the tag. The delay time determines the pulmonary vasculature depicted and can be manipulated to produce perfusion-type images (see Other Applications of ASL below). For pulmonary MR angiography, it is also possible to implement ASL by using a modified approach (109), whereby a spatially selective inversion pulse is applied in the area of interest, say in the coronal plane over the chest. Then, after an appropriate delay time for inflow, that same region is imaged. Although background signal is present in the chest wall and mediastinum, the depiction of the pulmonary vessels with this single acquisition can be excellent (Fig 23).

Carotid MR angiography.—Fast-flowing carotid arteries can be depicted by using balanced SSFP with ASL and combined with parallel imaging. In one implementation reported in abstract form, a nonselective inversion pulse and selective inversion pulse over the myocardium are applied in quick succession. After an inversion time selected to allow the tagged myocardial blood to fill the carotid arteries, the tagged protons are imaged by using a balanced SSFP sequence (113) (Fig 24). Clinical testing of this method in patients is needed.

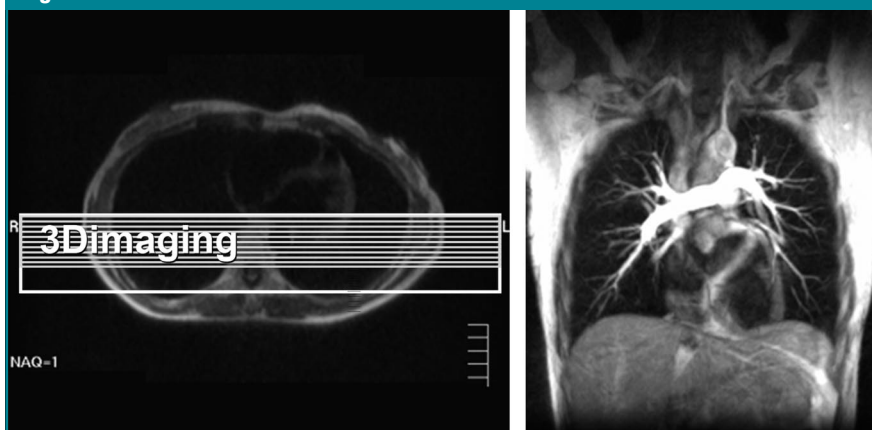
Renal MR angiography.—The balanced SSFP sequence is fully flow compensated in all three directions; therefore, complex orientation of the aorta relative to the renal arteries can be well depicted by using the technique (Fig 25). For renal MR angiography, similar work (111) has been reported by using a real-time navigator echo during free breathing, where both a tag-on and tag-off acquisition were used. Spuentrup et al used a cylindrical (pencil beam) 2D selective inversion pulse to tag the suprarenal aorta and a 350–450-msec delay from labeling to data acquisition, with a 122-msec acquisition to produce bright-blood renal MR angiography by using

balanced SSFP (111). In the initial clinical experience in eight healthy subjects and seven patients with renal artery stenosis, with subtraction of two navigator-gated data sets, results were comparable to contrast-enhanced MR angiographic images (111).

Distal-extremity MR angiography.—ASL with partial-Fourier FSE provides an alternative approach to ECG-gated 3D partial-Fourier FSE imaging. An example in the hand is shown in Figure 26. Acquisition of one tag-on and one tag-off scan (Fig 20), followed by the subtraction, eliminates background signal and improves visualization of small vessels in the hand and fingers. In Figure 26a, tagging at the wrist is used to show arteries in the whole hand. The technique can be modified to study the detail of even smaller vessels in the fingers (Fig 26b) by tagging the palm.

Other applications of ASL.—In addition to being used to produce angiograms, ASL can provide quantitative and physiologic data about blood flow. The method has been validated for quantitative brain perfusion (for recent

Figure 23



a.

Figure 23: Nonenhanced pulmonary MR angiography in a 28-year-old female volunteer by using modified ASL approach and partial-Fourier FSE (five R-R intervals/80; 180° flip angle; inversion time, 800 msec with intermittent breathhold technique). (a) A spatially selective inversion pulse is applied in the coronal plane over the chest and after a delay time for inflow, the same region is imaged. (b) Signal in the pulmonary vessels on coronal MIP derives from the fresh untagged spins entering the slab. Note that signal from the background (muscle and fat) remains. (Image courtesy of F. Tateishi, Kumamoto Central Hospital, Japan.)

b.

Figure 24

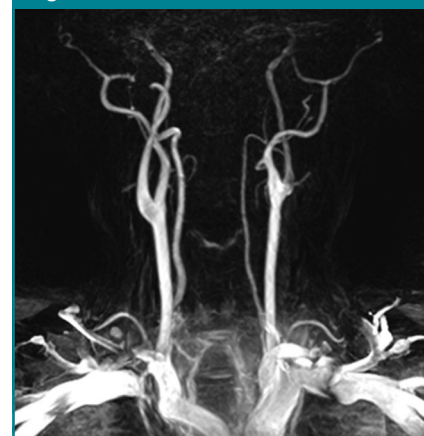


Figure 24: Nonenhanced carotid MR angiogram in a 34-year-old male volunteer by using ASL with balanced SSFP and parallel imaging (5/2.5; 120° flip angle; inversion time, 900 msec; peripheral pulse gating; parallel imaging factor, two). Alternating acquisitions with tag-on and tag-off (Fig 19) are used. Note that strong sensitivity to susceptibility with balanced SSFP causes signal loss in the subclavian arteries. (Image courtesy of Yuichi Yamashita, Toshiba.)

Figure 25

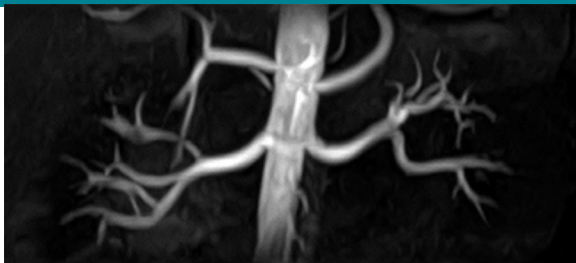


Figure 25: Nonenhanced renal MR angiogram in a 27-year-old male volunteer by using ASL with balanced SSFP (5.0/2.5; 120° flip angle; inversion time, 1100 msec; parallel imaging factor, two). Selective and nonselective tagging approach (Fig 20) was used for aortic inflow with an inferior presaturation pulse to eliminate venous flow. Acquisition was performed with respiratory triggering for a total scan time of 4 minutes. Frontal MIP is shown. (Image courtesy of J. Takahashi, Toranomon Hospital, Japan.)

reviews, see references 114,115). Measurement of blood velocity is also possible with ASL. For example, by knowing the distance between the tagged and imaging slabs and the total duration of time between application of the tag and collection of the image (inversion recovery time plus effective echo time), the mean blood velocity can be determined (109,116).

ASL methods can also be used to obtain noncontrast perfusion-like images outside the brain by varying the time delays between tagging and imaging, such as in the kidneys (108,117), lungs (118,119), and portal veins (120,121). Figure 27 illustrates a series of pulmonary MR angiographic images by using a range of time delays, from 300 to 2500 msec, following tagging of the heart blood. For delay times of 300–1000 msec, blood can be seen to flow from the pulmonary arteries to lung parenchyma, while after delay times of more than 1500 msec, blood begins to exit the lung parenchyma, causing decreasing signal.

Limitations

All techniques that rely on ASL for visualization of vessels share certain limitations. Because the technique relies on the replacement of blood in the imaging volume with tagged blood, the method requires reasonably high arterial velocity for success. In peripheral arteries, where blood velocity is slower, the time needed to replace the blood in the imaging volume can approach that of T1 recovery times for blood, resulting in loss

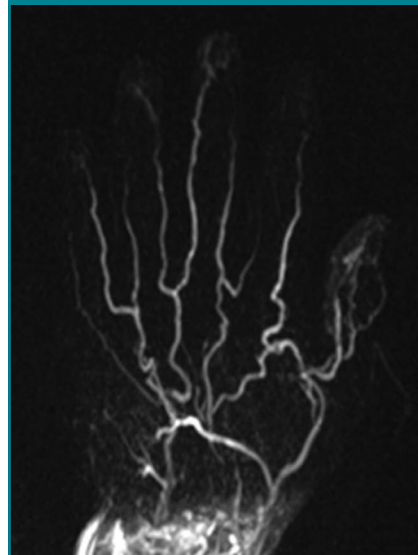
of the tagging effect. Multiple, separate, thinner-slab acquisitions may be necessary and therefore less efficient. Also, with selective tagging pulses for ASL MR angiography, flow direction is presumed. For applications such as peripheral MR angiography where flow reversal is sometimes encountered, this technique can be limited (akin to the problem of TOF with traveling saturation bands). Limitations of standard ASL methods that require subtraction of tagged and untagged datasets include longer acquisition times and the potential for motion between acquisitions to cause artifacts.

When implemented with ASL, partial-Fourier FSE and balanced SSFP methods have different advantages and disadvantages. To make bright-blood-tagged images with partial-Fourier FSE, the readout should be made during diastole, which lengthens the acquisition time, compared with balanced SSFP images, which can be acquired at any time without cardiac gating. On the other hand, balanced SSFP is much more strongly affected by susceptibility, compared with partial-Fourier FSE methods. For tortuous vessels or those with branches in different directions, the SSFP techniques may be preferable because the sequences are intrinsically flow compensated in three directions.

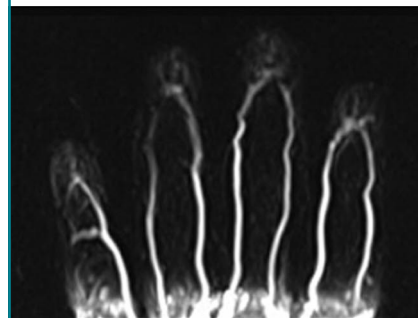
Summary of Applications for Different Vascular Territories

From the above discussion, clearly the differences in key characteristics and

Figure 26



a.



b.

Figure 26: Nonenhanced MR angiograms of the hand and digits in a 27-year-old male volunteer by using ASL and partial-Fourier FSE (three R-R intervals/80; 180° flip angle; inversion time, 600 msec). Alternating acquisitions with tag-on and tag-off (Fig 20) were used to image (a) the whole hand by applying the tag on the wrist and (b) the digits by applying the tag on the palm. (Image courtesy of J. Isogai, Hasuda Hospital, Japan.)

imaging requirements of different MR angiographic applications demand different nonenhanced strategies. A summary of possible strategies for nonenhanced MR angiography in different arterial territories is provided in the Table.

Future Directions

Imaging at field strengths higher than the conventional 1.5 T, such as with the

Figure 27

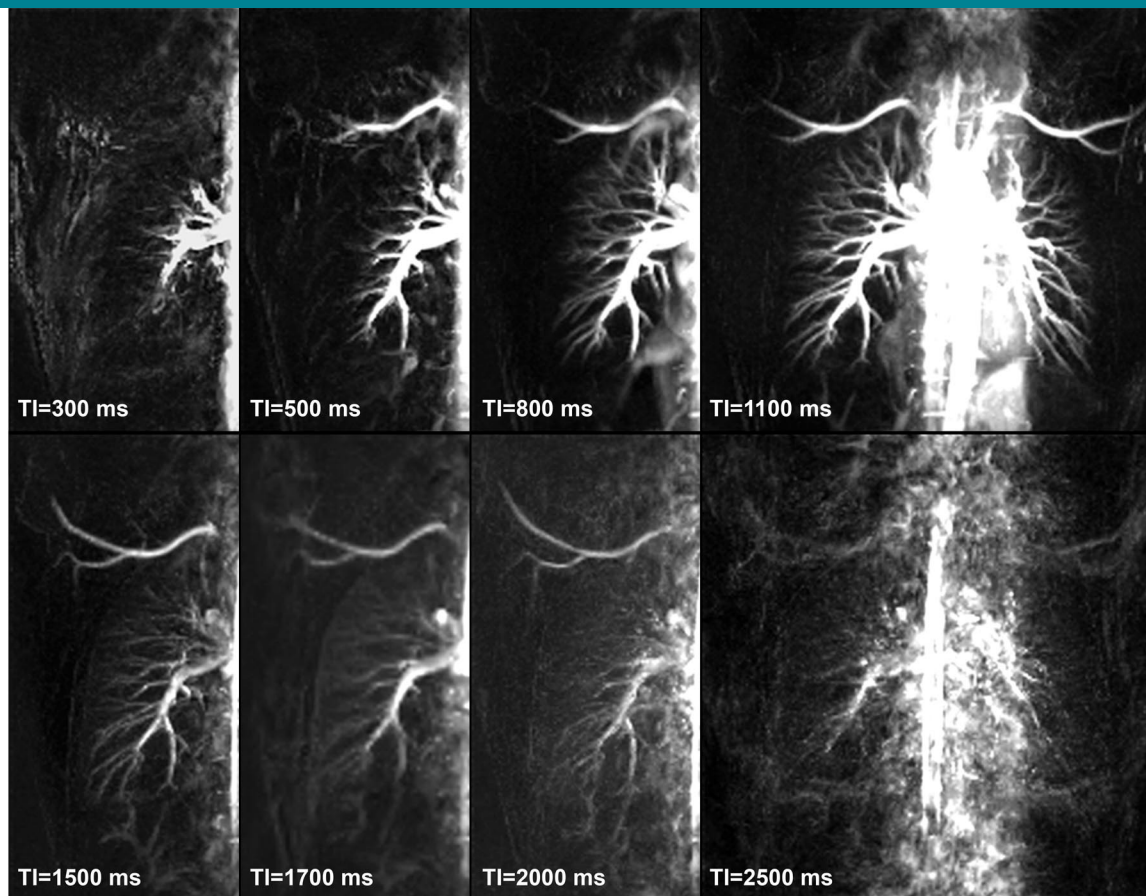


Figure 27: Perfusion-like images of the lungs in a 28-year-old female volunteer by using ASL technique with partial-Fourier FSE. Images acquired across a range of increasing inversion times (T_I) by using a sagittal tagging slab. Increasing inversion time allows the tagged blood to travel further into the periphery of the lungs. Note that background signal is canceled out by the subtraction of tag-on and tag-off images.

Suggested Nonenhanced MR Angiographic Techniques

MR Angiographic Application	MR Method	Notes*
Intracranial	3D TOF	TONE and MOTSA improve sensitivity to slower flow
Carotid	ASL with 3D balanced SSFP or partial-Fourier FSE, alternatively 2D or 3D TOF	...
Thoracic aorta	ECG-gated 3D partial-Fourier FSE alternatively 3D balanced SSFP	No flow spoiling, balanced SSFP can also be performed with ASL
Pulmonary	ECG-gated 3D partial-Fourier FSE alternatively ASL with 3D partial-Fourier FSE	Triggering in diastole
Coronary	ECG-gated 3D balanced SSFP	Breath hold alternatively navigator-free breathing
Abdominal aorta or renal	ASL with 3D balanced SSFP alternatively phase contrast	Multidirectional flow pattern favors SSFP over gated FSE
Peripheral	ECG-gated 3D partial-Fourier FSE with flow spoiling or flow compensation alternatively 2D TOF with traveling saturation bands	Customize degree of flow spoiling or compensation at each station
Hand and foot	ASL with 3D balanced SSFP or partial-Fourier FSE	Partial-Fourier FSE depicts morphology, ASL is a function of blood flow
Flow quantification	Phase contrast	...

* MOTSA = multiple overlapping thin slab acquisition, TONE = tilt optimized nonsaturated excitation.

Figure 28



Figure 28: Nonenhanced whole-body MR angiography at 1.5 T in a 39-year-old healthy male volunteer by using 3D ECG-gated partial-Fourier FSE (three R-R intervals/30; 180° flip angle; intermittent breathhold; total acquisition time, approximately 3 minutes per station). Images obtained with (a) a whole-body coil without parallel imaging and (b) 128-element coils with parallel imaging factor of six to eight (by implementation in both phase-encoding and section directions) in upper body and abdomen. Note less blurring in b (inset), compared with a (inset). (Image courtesy of Nobuyasu Ichinose, Toshiba, Japan.)

increasingly available 3-T systems, has different benefits and drawbacks for the various nonenhanced MR techniques. Longer T1 relaxation times inherently benefit ASL methods by prolonging the duration of tagging effects. However, if performed in conjunction with balanced SSFP methods, these advantages may be offset by the increased susceptibility at higher field strengths with balanced SSFP. On the other hand, improved arterial-venous contrast at 3 T can be achieved with balanced SSFP sequences by use of longer repetition time, which results in less conspicuous venous signal intensity on peripheral MR angiograms, and with the advantages of facilitating higher spatial resolution and reduced

bandwidths (33,96). For partial-Fourier FSE methods, specific absorption rate limitations may limit the use of full 180° refocusing pulses and result in reduced image contrast and signal-to-noise ratios. Nevertheless, the intrinsically higher signal-to-noise ratio at 3 T does lend itself well to the use of parallel imaging.

Implementation of parallel imaging can be particularly beneficial to nonenhanced MR angiographic methods by reducing acquisition times and consequently decreasing undesirable blurring and motion artifacts. Most applications of parallel imaging suffer a trade-off of reduced signal for shorter scan times; however, partial-Fourier FSE with parallel imaging allows for compensating

benefits that include a reduction in T2 blurring. With shorter acquisition times, multistation imaging with nonenhanced methods becomes feasible. An example of whole-body nonenhanced MR angiography with high parallel imaging factors is presented in Figure 28.

Last, a promising direction on the horizon is the development of time-resolved imaging techniques with nonenhanced MR angiographic methods, particularly the ECG-gated partial-Fourier FSE method (122) and ASL with SSFP (123). Time-resolved methods may become possible with higher order parallel imaging implemented with undersampling techniques that use methods such as radial imaging to vastly shorten ac-

quisition times (124). Use of incremental trigger delay times may allow improved sensitivity to a wider range of flow velocities and resemble time-resolved contrast-enhanced MR angiography (Fig 29). Initial data suggest that delays in enhancement on the time-resolved images may reflect the severity of stenosis in peripheral vascular disease (92), a promising indication of advances to come in nonenhanced MR angiography.

Glossary

arterial spin labeling, or ASL

MR imaging technique where protons in a specific region, typically in a blood vessel upstream of the imaging field of view, experience an inversion pulse and are thereby “tagged.” After a fixed interval, or delay time, when the tagged protons have traveled into the field of view, imaging is performed. Variations on this approach can also be performed to suppress undesired background signal through additional nonselective inversion pulses.

balanced steady-state free precession, or SSFP

A gradient-echo sequence frequently used in cardiovascular applications where signal intensity does not depend on blood flow but rather on the ratio of T2 to T1 relaxation times; blood is typically bright. Also referred to as fast imaging employing steady-state acquisition, or FIESTA, true fast imaging with steady-state precession, or true FISP, balanced fast field echo, or balanced FFE.

fast spin echo, or FSE

A spin-echo sequence that uses multiple 180° refocusing pulses to generate a number of spin echoes per radiofrequency excitation. The number of spin echoes is referred to as the echo train length, and the time between consecutive echoes is the echo train spacing.

flow compensation

Technique designed to reduce the signal loss or dephasing caused by blood moving with constant velocity. The method relies on specially designed positive and negative gradients applied in the direc-

tion of blood flow. Also referred to as gradient moment nulling.

inversion pulse

A 180° radiofrequency pulse that serves to invert the longitudinal magnetization. Inversion pulses are used as prepulses for sequences such as short tau inversion recovery (STIR) that are designed to null signal from fat. They are also used in ASL sequences where protons used for imaging are selectively “tagged” by using inversion pulses.

magnetization transfer

The transfer of energy between free, unbound water protons and protons bound to macromolecules that results in differences in T2 relaxation times. Magnetization transfer is used to suppress background tissue, such as brain parenchyma, to allow greater conspicuity of vessels.

multiple overlapping thin-slab acquisition, or MOTSA

A TOF angiographic method that uses multiple thin 3D slabs, which slightly overlap, so that the resulting overall 3D angiogram has less signal saturation than would occur with a single-volume 3D acquisition.

parallel imaging

A technique for undersampling k-space by using coil sensitivity profiles, which results in substantial reductions in acquisition times at a cost of reduced signal-to-noise ratios.

partial Fourier

A term used to refer to incomplete filling of k-space by using a reduced number of phase-encoding steps to shorten acquisition times.

phase-contrast angiography

A technique for generating MR angiograms that relies on the accumulation of phase differences as moving protons travel through magnetic field gradients.

short tau inversion recovery, or STIR

A fat-suppression technique that uses an inversion recovery pulse with an inversion time selected to null the signal from fat.

Figure 29

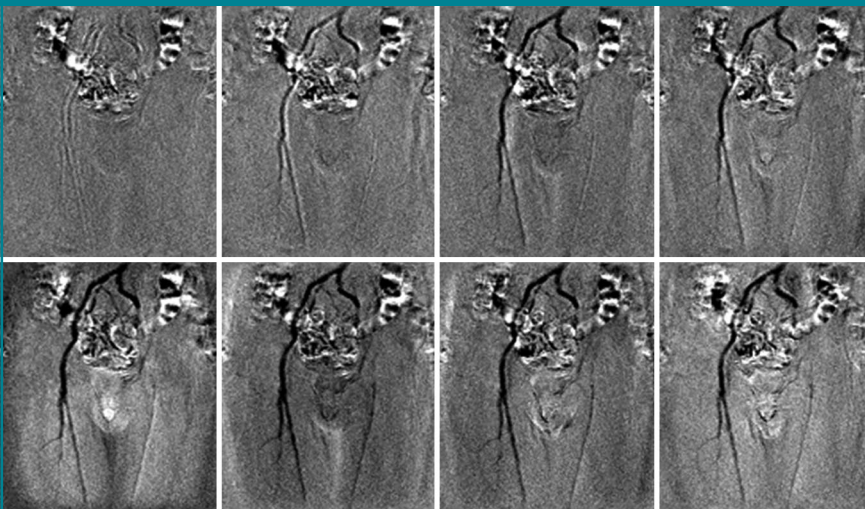


Figure 29: Time-resolved nonenhanced MR angiograms in a 62-year-old male patient with arteriosclerosis obliterans at occlusion of the left external artery by using 2D single-shot partial-Fourier FSE (three R-R intervals/80 effective, 180° refocusing flip angle) with incremental delay times. Selected images are depicted from a series acquired with delay time increments of 10 msec and subtraction of systolic images from diastolic images. From late systolic to diastolic phases, images show normal flow in the right iliac artery, whereas the left iliac artery shows delay in flow due to stenosis. (Image courtesy of Dr. K. Nakamura, Kyoritsu Tobata Hospital, Japan.)

spatially selective excitation pulses

Radiofrequency pulses that are applied to specific regions of the body so as to result in excitation of only protons in those regions, without affecting the remainder of the protons in the field of view.

spoiler gradients

Extended application of gradients to dephase magnetization. In the case of ECG-gated 3D partial-Fourier FSE sequences, the spoiler gradients are used to enhance differences between arterial and venous blood signal.

tilt optimized nonsaturated excitation, or TONE

Technique used for intracranial TOF MR angiography to compensate for saturation of blood flowing into the imaging slab by using progressively increasing flip angles to image protons that have moved deeper into the slab.

time-of-flight angiography

MR angiography technique based on the differences between protons in stationary tissue, which are saturated by repeated radiofrequency excitations and the high signal from fresh unsaturated protons that move into the imaging slab between each excitation pulse.

time-resolved angiography

A term used to refer to repeated MR angiographic acquisitions that depict the temporal changes related to the arrival and passage of blood through the arterial and venous systems.

References

- Prince MR. Gadolinium-enhanced MR aortography. *Radiology* 1994;191:155–164.
- Wilman AH, Riederer SJ, King BF, Debbins JP, Rossman PJ, Ehman RL. Fluoroscopically triggered contrast-enhanced three-dimensional MR angiography with elliptical centric view order: application to the renal arteries. *Radiology* 1997;205:137–146.
- Earls JP, Rofsky NM, DeCorato DR, Krinsky GA, Weinreb JC. Breath-hold single-dose gadolinium-enhanced three-dimensional MR aortography: usefulness of a timing examination and MR power injector. *Radiology* 1996;201:705–710.
- Kita M, Mitani Y, Tanihata H, et al. Moving-table reduced-dose gadolinium-enhanced three-dimensional magnetic resonance angiography: velocity-dependent method with three-phase gadolinium infusion. *J Magn Reson Imaging* 2001;14:319–328.
- Ho KY, Leiner T, de Haan MW, Kessels AG, Kitslaar PJ, van Engelshoven JM. Peripheral vascular tree stenoses: evaluation with moving-bed infusion-tracking MR angiography. *Radiology* 1998;206:683–692.
- Meaney JF, Ridgway JP, Chakraverty S, et al. Stepping-table gadolinium-enhanced digital subtraction MR angiography of the aorta and lower extremity arteries: preliminary experience. *Radiology* 1999;211:59–67.
- Sodickson DK, McKenzie CA, Li W, Wolff S, Manning WJ, Edelman RR. Contrast-enhanced 3D MR angiography with simultaneous acquisition of spatial harmonics: a pilot study. *Radiology* 2000;217:284–289.
- Korosec FR, Frayne R, Grist TM, Mistretta CA. Time-resolved contrast-enhanced 3D MR angiography. *Magn Reson Med* 1996;36:345–351.
- Wildermuth S, Debatin JF, Huisman TA, Leung DA, McKinnon GC. 3D phase contrast EPI MR angiography of the carotid arteries. *J Comput Assist Tomogr* 1995;19:871–878.
- Miller S, Schick F, Duda SH, et al. Gd-enhanced 3D phase-contrast MR angiography and dynamic perfusion imaging in the diagnosis of renal artery stenosis. *Magn Reson Imaging* 1998;16:1005–1012.
- Dumoulin CL, Yucel EK, Vock P, et al. Two- and three-dimensional phase contrast MR angiography of the abdomen. *J Comput Assist Tomogr* 1990;14:779–784.
- Dumoulin CL, Souza SP, Walker MF, Wagle W. Three-dimensional phase contrast angiography. *Magn Reson Med* 1989;9:139–149.
- Nishimura DG, Macovski A, Pauly JM, Conolly SM. MR angiography by selective inversion recovery. *Magn Reson Med* 1987;4:193–202.
- Edelman RR, Siewert B, Adamis M, Gaa J, Laub G, Wielopolski P. Signal targeting with alternating radiofrequency (STAR) sequences: application to MR angiography. *Magn Reson Med* 1994;31:233–238.
- Wielopolski PA, Adamis M, Prasad P, Gaa J, Edelman R. Breath-hold 3D STAR MR angiography of the renal arteries using segmented echo planar imaging. *Magn Reson Med* 1995;33:432–438.
- Sodickson DK, Manning WJ. Simultaneous acquisition of spatial harmonics (SMASH): fast imaging with radiofrequency coil arrays. *Magn Reson Med* 1997;38:591–603.
- Pruessmann KP, Weiger M, Scheidegger MB, Boesiger P. SENSE: sensitivity encoding for fast MRI. *Magn Reson Med* 1999;42:952–962.
- Cowper SE, Robin HS, Steinberg SM, Su LD, Gupta S, LeBoit PE. Scleromyxoidema-like cutaneous diseases in renal-dialysis patients. *Lancet* 2000;356:1000–1001.
- Sadowski EA, Bennett LK, Chan MR, et al. Nephrogenic systemic fibrosis: risk factors and incidence estimation. *Radiology* 2007;243:148–157.
- Grobner T. Gadolinium: a specific trigger for the development of nephrogenic fibrosing dermopathy and nephrogenic systemic fibrosis? *Nephrol Dial Transplant* 2006;21:1104–1108. [Published correction appears in *Nephrol Dial Transplant* 2006;21:1745.]
- Urata J, Miyazaki M, Wada H, Nakaura T, Yamashita Y, Takahashi M. Clinical evaluation of aortic diseases using nonenhanced MRA with ECG-triggered 3D half-Fourier FSE. *J Magn Reson Imaging* 2001;14:113–119.
- Lee VS, Martin DJ, Krinsky GA, Rofsky NM. Gadolinium-enhanced MR angiography: artifacts and pitfalls. *AJR Am J Roentgenol* 2000;175:197–205.
- Lohan DG, Saleh R, Nael K, Krishnam M, Finn JP. Contrast-enhanced MRA versus nonenhanced MRA: pros and cons. *Appl Radiol* 2007;36(suppl):3–15.
- Kanda T, Nakamura E, Moritani T, Yamori Y. Arterial pulse wave velocity and risk factors for peripheral vascular disease. *Eur J Appl Physiol* 2000;82:1–7.
- Rose SC. Noninvasive vascular laboratory for evaluation of peripheral arterial occlusive disease. II. Clinical applications: chronic, usually atherosclerotic, lower extremity ischemia. *J Vasc Interv Radiol* 2000;11:1257–1275.
- Fronek A, Coel M, Berstein EF. Quantitative ultrasonographic studies of lower extremity flow velocities in health and disease. *Circulation* 1976;53:957–960.
- Toursarkissian B, Mejia A, Smilanich RP, Schoolfield J, Shireman PK, Sykes MT. Noninvasive localization of infrainguinal arterial occlusive disease in diabetics. *Ann Vasc Surg* 2001;15:73–78.
- Parker DL, Tsuruda JS, Goodrich KC, Alexander AL, Buswell HR. Contrast-enhanced magnetic resonance angiography of cerebral arteries: a review. *Invest Radiol* 1998;33:560–572.

29. Bernstein MA, Huston J 3rd, Lin C, Gibbs GF, Felmlee JP. High-resolution intracranial and cervical MRA at 3.0T: technical considerations and initial experience. *Magn Reson Med* 2001;46:955-962.
30. de Bazelaire CM, Duhamel GD, Rofsky NM, Alsop DC. MR imaging relaxation times of abdominal and pelvic tissues measured in vivo at 3.0 T: preliminary results. *Radiology* 2004;230:652-659.
31. Barth M, Moser E. Proton NMR relaxation times of human blood samples at 1.5 T and implications for functional MRI. *Cell Mol Biol (Noisy-le-grand)* 1997;43:783-791.
32. Wright GA, Hu BS, Macovski A. 1991 I.I. Rabi Award. Estimating oxygen saturation of blood in vivo with MR imaging at 1.5 T. *J Magn Reson Imaging* 1991;1:275-283.
33. Brittain JH, Olcott EW, Szuba A, et al. Three-dimensional flow-independent peripheral angiography. *Magn Reson Med* 1997;38:343-354.
34. Gronas R, Kalman PG, Kucey DS, Wright GA. Flow-independent angiography for peripheral vascular disease: initial in-vivo results. *J Magn Reson Imaging* 1997;7:637-643.
35. Pomposelli FB, Kansal N, Hamdan AD, et al. A decade of experience with dorsalis pedis artery bypass: analysis of outcome in more than 1000 cases. *J Vasc Surg* 2003;37:307-315.
36. Hughes K, Domenig CM, Hamdan AD, et al. Bypass to plantar and tarsal arteries: an acceptable approach to limb salvage. *J Vasc Surg* 2004;40:1149-1157.
37. Hahn WY, Hecht EM, Friedman B, Babb JS, Jacobowitz GR, Lee VS. Distal lower extremity imaging: prospective comparison of 2-dimensional time of flight, 3-dimensional time-resolved contrast-enhanced magnetic resonance angiography, and 3-dimensional bolus chase contrast-enhanced magnetic resonance angiography. *J Comput Assist Tomogr* 2007;31:29-36.
38. Masaryk TJ, Laub GA, Modic MT, Ross JS, Haacke EM. Carotid-CNS MR flow imaging. *Magn Reson Med* 1990;14:308-314.
39. Laub GA. Time-of-flight method of MR angiography. *Magn Reson Imaging Clin N Am* 1995;3:391-398.
40. Kaufman JA, McCarter D, Geller SC, Waltman AC. Two-dimensional time-of-flight MR angiography of the lower extremities: artifacts and pitfalls. *AJR Am J Roentgenol* 1998;171:129-135.
41. Li W, Zhang M, Sher S, Edelman RR. MR angiography of the vascular tree from the aorta to the foot: combining two-dimensional time-of-flight and three-dimensional contrast-enhanced imaging. *J Magn Reson Imaging* 2000;12:884-889.
42. Nelemans PJ, Leiner T, de Vet HC, van Engelshoven JM. Peripheral arterial disease: meta-analysis of the diagnostic performance of MR angiography. *Radiology* 2000;217:105-114.
43. Owen RS, Carpenter JP, Baum RA, Perloff LJ, Cope C. Magnetic resonance imaging of angiographically occult runoff vessels in peripheral arterial occlusive disease. *N Engl J Med* 1992;326:1577-1581.
44. McCauley TR, Monib A, Dickey KW, et al. Peripheral vascular occlusive disease: accuracy and reliability of time-of-flight MR angiography. *Radiology* 1994;192:351-357.
45. Carpenter JP, Baum RA, Holland GA, Barker CF. Peripheral vascular surgery with magnetic resonance angiography as the sole preoperative imaging modality. *J Vasc Surg* 1994;20:861-869; discussion 869-871.
46. Baum RA, Rutter CM, Sunshine JH, et al. Multicenter trial to evaluate vascular magnetic resonance angiography of the lower extremity. American College of Radiology Rapid Technology Assessment Group. *JAMA* 1995;274:875-880.
47. Atkinson D, Brant-Zawadzki M, Gillan G, Purdy D, Laub G. Improved MR angiography: magnetization transfer suppression with variable flip angle excitation and increased resolution. *Radiology* 1994;190:890-894.
48. Blatter DD, Parker DL, Robinson RO. Cerebral MR angiography with multiple overlapping thin slab acquisition. *Radiology* 1991;179:805-811.
49. Parker DL, Yuan C, Blatter DD. MR angiography by multiple thin slab 3D acquisition. *Magn Reson Med* 1991;17:434-451.
50. Pike GB, Hu BS, Glover GH, Enzmann DR. Magnetization transfer time-of-flight magnetic resonance angiography. *Magn Reson Med* 1992;25:372-379.
51. Miyazaki M, Kojima F, Ichinose N, Onozato Y, Igarashi H. A novel saturation transfer contrast method for 3D time-of-flight magnetic resonance angiography: a slice-selective off-resonance sinc pulse (SORS) technique. *Magn Reson Med* 1994;32:52-59.
52. Dumoulin CL. Phase contrast MR angiography techniques. *Magn Reson Imaging Clin N Am* 1995;3:399-411.
53. Steffens JC, Link J, Muller-Hulsbeck S, Freund M, Brinkmann G, Heller M. Cardiac-gated two-dimensional phase-contrast MR angiography of lower extremity occlusive disease. *AJR Am J Roentgenol* 1997;169:749-754.
54. Zhang H, Prince MR. Renal MR angiography. *Magn Reson Imaging Clin N Am* 2004;12:487-503, vi.
55. Meyers SP, Talagala SL, Totterman S, et al. Evaluation of the renal arteries in kidney donors: value of three-dimensional phase-contrast MR angiography with maximum-intensity-projection or surface rendering. *AJR Am J Roentgenol* 1995;164:117-121.
56. de Haan MW, Kouwenhoven M, Thelissen RP, et al. Renovascular disease in patients with hypertension: detection with systolic and diastolic gating in three-dimensional, phase-contrast MR angiography. *Radiology* 1996;198:449-456.
57. De Cobelli F, Mellone R, Salvioni M, et al. Renal artery stenosis: value of screening with three-dimensional phase-contrast MR angiography with a phased-array multicoil. *Radiology* 1996;201:697-703.
58. Duda SH, Schick F, Teuffl F, et al. Phase-contrast MR angiography for detection of arteriosclerotic renal artery stenosis. *Acta Radiol* 1997;38:287-291.
59. De Cobelli F, Vanzulli A, Sironi S, et al. Renal artery stenosis: evaluation with breath-hold, three-dimensional, dynamic, gadolinium-enhanced versus three-dimensional, phase-contrast MR angiography. *Radiology* 1997;205:689-695.
60. Hahn U, Miller S, Nagele T, et al. Renal MR angiography at 1.0 T: three-dimensional (3D) phase-contrast techniques versus gadolinium-enhanced 3D fast low-angle shot breath-hold imaging. *AJR Am J Roentgenol* 1999;172:1501-1508.
61. Prince MR, Schoenberg SO, Ward JS, Londy FJ, Wakefield TW, Stanley JC. Hemodynamically significant atherosclerotic renal artery stenosis: MR angiographic features. *Radiology* 1997;205:128-136.
62. Reimer P, Boos M. Phase-contrast MR angiography of peripheral arteries: technique and clinical application. *Eur Radiol* 1999;9:122-127.
63. Nghiem HV, Winter TC 3rd, Mountford MC, et al. Evaluation of the portal venous system before liver transplantation: value of phase-contrast MR angiography. *AJR Am J Roentgenol* 1995;164:871-878.
64. Gu T, Korosec FR, Block WF, et al. PC VIPR: a high-speed 3D phase-contrast method for flow quantification and high-resolution angiography. *AJNR Am J Neuroradiol* 2005;26:743-749.
65. Wentland AL, Korosec FR, Vigen KK, Wieben O, Fine JP, Grist TM. Cine flow

- measurements using phase contrast with undersampled projections: in vitro validation and preliminary results in vivo. *J Magn Reson Imaging* 2006;24:945-951.
66. Liu Y, Karonen JO, Vanninen RL, et al. Acute ischemic stroke: predictive value of 2D phase-contrast MR angiography—serial study with combined diffusion and perfusion MR imaging. *Radiology* 2004;231:517-527.
 67. Iseda T, Nakano S, Miyahara D, Uchinokura S, Goya T, Wakisaka S. Poststenotic signal attenuation on 3D phase-contrast MR angiography: a useful finding in haemodynamically significant carotid artery stenosis. *Neuroradiology* 2000;42:868-873.
 68. Vanninen RL, Manninen HI, Partanen PL, Vainio PA, Soimakallio S. Carotid artery stenosis: clinical efficacy of MR phase-contrast flow quantification as an adjunct to MR angiography. *Radiology* 1995;194:459-467.
 69. Forster BB, Johnstone RD, Shannon HM, et al. Quantification of hemodynamic improvement after superficial femoral artery angioplasty by cine phase contrast MR angiography. *AJR Am J Roentgenol* 1999;173:1564-1566.
 70. Mohajer K, Zhang H, Gurell D, et al. Superficial femoral artery occlusive disease severity correlates with MR cine phase-contrast flow measurements. *J Magn Reson Imaging* 2006;23:355-360.
 71. Debatin JF, Ting RH, Wegmuller H, et al. Renal artery blood flow: quantitation with phase-contrast MR imaging with and without breath holding. *Radiology* 1994;190:371-378.
 72. Silverman JM, Friedman ML, Van Allan RJ. Detection of main renal artery stenosis using phase-contrast cine MR angiography. *AJR Am J Roentgenol* 1996;166:1131-1137.
 73. Masui T, Takehara Y, Igarashi T, et al. MR angiography of the renal artery: comparison of breath-hold two-dimensional phase-contrast cine technique with the phased-array coil and breath-hold two-dimensional time-of-flight technique with the body coil. *Eur J Radiol* 1997;25:62-66.
 74. Wasser MN, Westenberg J, van der Hulst VP, et al. Hemodynamic significance of renal artery stenosis: digital subtraction angiography versus systolically gated three-dimensional phase-contrast MR angiography. *Radiology* 1997;202:333-338.
 75. Schoenberg SO, Knopp MV, Bock M, et al. Renal artery stenosis: grading of hemodynamic changes with cine phase-contrast MR blood flow measurements. *Radiology* 1997;203:45-53.
 76. Lee VS, Rofsky NM, Ton AT, Johnson G, Krinsky GA, Weinreb JC. Angiotensin-converting enzyme inhibitor-enhanced phase-contrast MR imaging to measure renal artery velocity waveforms in patients with suspected renovascular hypertension. *AJR Am J Roentgenol* 2000;174:499-508.
 77. de Haan MW, Kouwenhoven M, Kessels AG, van Engelshoven JM. Renal artery blood flow: quantification with breath-hold or respiratory triggered phase-contrast MR imaging. *Eur Radiol* 2000;10:1133-1137.
 78. Silverman JM, Raissi S, Tyszka JM, Trento A, Herfkens RJ. Phase-contrast cine MR angiography detection of thoracic aortic dissection. *Int J Card Imaging* 2000;16:461-470.
 79. Julsrud PR, Breen JF, Felmlee JP, Warnes CA, Connolly HM, Schaff HV. Coarctation of the aorta: collateral flow assessment with phase-contrast MR angiography. *AJR Am J Roentgenol* 1997;169:1735-1742.
 80. Kato T, Indo T, Yoshida E, Iwasaki Y, Sone M, Sobue G. Contrast-enhanced 2D cine phase MR angiography for measurement of basilar artery blood flow in posterior circulation ischemia. *AJNR Am J Neuroradiol* 2002;23:1346-1351.
 81. Sanz J, Kuschner P, Rius T, et al. Pulmonary arterial hypertension: noninvasive detection with phase-contrast MR imaging. *Radiology* 2007;243:70-79.
 82. Grinstead JW, Sinha S, Tateshima S, Nien YL, Vinuela F. Visualization and quantification of flow and velocity fields in intracranial arteriovenous malformations using phase-contrast MR angiography. *AJR Am J Roentgenol* 2006;186:553-555.
 83. Wedeen VJ, Meuli RA, Edelman RR, et al. Projective imaging of pulsatile flow with magnetic resonance. *Science* 1985;230:946-948.
 84. Meuli RA, Wedeen VJ, Geller SC, et al. MR gated subtraction angiography: evaluation of lower extremities. *Radiology* 1986;159:411-418.
 85. Miyazaki M, Sugiura S, Tateishi F, Wada H, assai Y, Abe H. Non-contrast-enhanced MR angiography using 3D ECG-synchronized half-Fourier fast spin echo. *J Magn Reson Imaging* 2000;12:776-783.
 86. Miyazaki M, Takai H, Sugiura S, Wada H, Kuwahara R, Urata J. Peripheral MR angiography: separation of arteries from veins with flow-spoiled gradient pulses in electrocardiography-triggered three-dimensional half-Fourier fast spin-echo imaging. *Radiology* 2003;227:890-896.
 87. Axel L, Morton D. MR flow imaging by velocity-compensated/uncompensated difference images. *J Comput Assist Tomogr* 1987;11:31-34.
 88. Constable RT, Gore JC. The loss of small objects in variable TE imaging: implications for FSE, RARE, and EPI. *Magn Reson Med* 1992;28:9-24.
 89. Hinks RS, Constable RT. Gradient moment nulling in fast spin echo. *Magn Reson Med* 1994;32:698-706.
 90. Urata J, Wada H, Kuwahara R, Miyazaki M, Nishiharu T, Yamashita Y. Evaluation of lower extremity arterial diseases using flow-dephasing spoiler gradient pulses in ECG-triggered 3D half-Fourier FSE: initial experience [abstr]. In: Proceedings of the Tenth Meeting of the International Society for Magnetic Resonance in Medicine. Berkeley, Calif: International Society for Magnetic Resonance in Medicine, 2002; 1750.
 91. Lim RP, Hecht EM, Xu J, et al. 3D Non-gadolinium enhanced ECG-gated MRA of the distal lower extremities: preliminary clinical experience. *J Magn Reson Imaging* (in press).
 92. Nakamura K, Kuroki K, Yamamoto A, Hiramane A, Miyazaki M, Matsufuji Y. Fresh blood imaging (FBI) of peripheral arteries: comparison with 16-detector row CT angiography [abstr]. In: Proceedings of the Fourteenth Meeting of the International Society for Magnetic Resonance in Medicine. Berkeley, Calif: International Society for Magnetic Resonance in Medicine, 2006; 1929.
 93. Carr HY. Steady-state free precession in nuclear magnetic resonance. *Phys Rev* 1958;112:1693-1701.
 94. Scheffler K, Lehnhardt S. Principles and applications of balanced SSFP techniques. *Eur Radiol* 2003;13:2409-2418.
 95. Coenegrachts KL, Hoogeveen RM, Vaninbrouck JA, et al. High-spatial-resolution 3D balanced turbo field-echo technique for MR angiography of the renal arteries: initial experience. *Radiology* 2004;231:237-242.
 96. Brittain JH, Shimakawa A, Johnson JW, et al. SSFP Non-contrast-enhanced MR angiography at 3.0T: improved arterial-venous contrast with increased TR [abstr]. In: Proceedings of the Thirteenth Meeting of the International Society for Magnetic Resonance in Medicine. Berkeley, Calif: International Society for Magnetic Resonance in Medicine, 2005; 1708.

97. Deshpande VS, Shea SM, Laub G, Simonetti OP, Finn JP, Li D. 3D magnetization-prepared true-FISP: a new technique for imaging coronary arteries. *Magn Reson Med* 2001;46:494–502.
98. Shea SM, Deshpande VS, Chung YC, Li D. Three-dimensional true-FISP imaging of the coronary arteries: improved contrast with T2-preparation. *J Magn Reson Imaging* 2002;15:597–602.
99. Jahnke C, Paetsch I, Schnackenburg B, et al. Coronary MR angiography with steady-state free precession: individually adapted breath-hold technique versus free-breathing technique. *Radiology* 2004;232:669–676.
100. Niendorf T, Saranathan M, Lingamneni A, et al. Short breath-hold, volumetric coronary MR angiography employing steady-state free precession in conjunction with parallel imaging. *Magn Reson Med* 2005;53:885–894.
101. Sakuma H, Ichikawa Y, Suzawa N, et al. Assessment of coronary arteries with total study time of less than 30 minutes by using whole-heart coronary MR angiography. *Radiology* 2005;237:316–321.
102. Spuentrup E, Katoh M, Buecker A, et al. Free-breathing 3D steady-state free precession coronary MR angiography with radial k-space sampling: comparison with cartesian k-space sampling and cartesian gradient-echo coronary MR angiography—pilot study. *Radiology* 2004;231:581–586.
103. Wu YW, Tadamura E, Yamamuro M, Kanao S, Nakayama K, Togashi K. Evaluation of three-dimensional navigator-gated whole heart MR coronary angiography: the importance of systolic imaging in subjects with high heart rates. *Eur J Radiol* 2007;61:91–96.
104. Niendorf T, Hardy CJ, Giaquinto RO, et al. Toward single breath-hold whole-heart coverage coronary MRA using highly accelerated parallel imaging with a 32-channel MR system. *Magn Reson Med* 2006;56:167–176.
105. Stuber M, Bornert P, Spuentrup E, Botnar RM, Manning WJ. Selective three-dimensional visualization of the coronary arterial lumen using arterial spin tagging. *Magn Reson Med* 2002;47:322–329.
106. Katoh M, Stuber M, Buecker A, Gunther RW, Spuentrup E. Spin-labeling coronary MR angiography with steady-state free precession and radial k-space sampling: initial results in healthy volunteers. *Radiology* 2005;236:1047–1052.
107. Wehrli FW, Shimakawa A, MacFall JR, Axel L, Perman W. MR imaging of venous and arterial flow by a selective saturation-recovery spin echo (SSRSE) method. *J Comput Assist Tomogr* 1985;9:537–545.
108. Prasad PV, Kim D, Kaiser AM, et al. Non-invasive comprehensive characterization of real artery stenosis by combination of STAR angiography and EPISTAR perfusion imaging. *Magn Reson Med* 1997;38:776–787.
109. Kanazawa H, Miyazaki M. Time-spatial labeling inversion tag (t-SLIT) using a selective IR-tag on/off pulse in 2D and 3D half-Fourier FSE as arterial spin labeling [abstr]. In: Proceedings of the Tenth Meeting of the International Society for Magnetic Resonance in Medicine. Berkeley, Calif: International Society for Magnetic Resonance in Medicine, 2002; 140.
110. Katoh M, Buecker A, Stuber M, Gunther RW, Spuentrup E. Free-breathing renal MR angiography with steady-state free-precession (SSFP) and slab-selective spin inversion: initial results. *Kidney Int* 2004;66:1272–1278.
111. Spuentrup E, Manning WJ, Bornert P, Kissinger KV, Botnar RM, Stuber M. Renal arteries: navigator-gated balanced fast field-echo projection MR angiography with aortic spin labeling—initial experience. *Radiology* 2002;225:589–596.
112. Kurihara Y, Yakushiji Y, Nakashima Y, Higashi M, Miyazaki M. Non-contrast-enhanced selective MR pulmonary angiography using time-spatial labeling inversion tag pulse [abstr]. In: Proceedings of the Tenth Meeting of the International Society for Magnetic Resonance in Medicine. Berkeley, Calif: International Society for Magnetic Resonance in Medicine, 2002; 1781.
113. Yui M, Miyazaki M, Kanazawa H, Okamoto K. Aortic arch to intracranial 3D MRA with t-SLIT 3D-SSFP using a neurovascular-attached QD head SPEEDER coil [abstr]. In: Proceedings of the Twelfth Meeting of the International Society for Magnetic Resonance in Medicine. Berkeley, Calif: International Society for Magnetic Resonance in Medicine, 2004; 2121.
114. Williams DS. Quantitative perfusion imaging using arterial spin labeling. *Methods Mol Med* 2006;124:151–173.
115. Golay X, Hendrikse J, Lim TC. Perfusion imaging using arterial spin labeling. *Top Magn Reson Imaging* 2004;15:10–27.
116. Barbier EL, Silva AC, Kim SG, Koretsky AP. Perfusion imaging using dynamic arterial spin labeling (DASL). *Magn Reson Med* 2001;45:1021–1029.
117. Karger N, Biederer J, Lusse S, et al. Quantitation of renal perfusion using arterial spin labeling with FAIR-UFLARE. *Magn Reson Imaging* 2000;18:641–647.
118. Mai VM, Hagspiel KD, Altes T, Goode AR, Williams MB, Berr SS. Detection of regional pulmonary perfusion deficit of the occluded lung using arterial spin labeling in magnetic resonance imaging. *J Magn Reson Imaging* 2000;11:97–102.
119. Mai VM, Bankier AA, Prasad PV, et al. MR ventilation-perfusion imaging of human lung using oxygen-enhanced and arterial spin labeling techniques. *J Magn Reson Imaging* 2001;14:574–579.
120. Ito K, Koike S, Jo C, et al. Intraportal venous flow distribution: evaluation with single breath-hold ECG-triggered three-dimensional half-Fourier fast spin-echo MR imaging and a selective inversion-recovery tagging pulse. *AJR Am J Roentgenol* 2002;178:343–348.
121. Tsukuda T, Ito K, Koike S, et al. Pre- and postprandial alterations of portal venous flow: evaluation with single breath-hold three-dimensional half-Fourier fast spin-echo MR imaging and a selective inversion-recovery tagging pulse. *J Magn Reson Imaging* 2005;22:527–533.
122. Nakamura K, Yamamoto A, Kuroki K, Miyazaki M, Matsufuji Y. Flow-motion FBI: a novel non-contrast-enhanced 3D-MRDSA technique using ECG-triggered three-dimensional half-Fourier FSE—the feasibility to evaluate hemodynamics of peripheral vascular disease [abstr]. In: Proceedings of the Thirteenth Meeting of the International Society for Magnetic Resonance in Medicine. Berkeley, Calif: International Society for Magnetic Resonance in Medicine, 2005; 1713.
123. Yamashita Y, Yamamoto A, Suzuki M, Nomiya A, Aoki I, Yui M. Selective visualization of blood flow using SSFP non-contrast MRA with time-spatial labeling inversion pulse [abstr]. In: Proceedings of the Fourteenth Meeting of the International Society for Magnetic Resonance in Medicine. Berkeley, Calif: International Society for Magnetic Resonance in Medicine, 2006; 1928.
124. Mistretta CA, Wieben O, Velikina J, et al. Highly constrained backprojection for time-resolved MRI. *Magn Reson Med* 2006;55:30–40.